High-throughput transposon sequencing highlights cell wall as an important barrier for osmotic stress in methicillin resistant *Staphylococcus aureus* and underlines a tailored response to different osmotic stressors

Short Title: Global analysis of osmotic stress responses in Staphylococcus aureus

Christopher F. Schuster[a], David M. Wiedemann[a], Freja C. M. Kirsebom[a,1], Marina Santiago[b,2], Suzanne Walker[b] and Angelika Gründling[a,3]

ORCID IDs: 0000-0002-4566-7226 (CFS), 0000-0001-6961-0980 (DMW), 0000-0003-4585-319X (FCK), 0000-0002-5446-3452 (MS), 0000-0002-0545-914X (SW), 0000-0002-6235-8687 (AG)

[a]Section of Microbiology and MRC Centre for Molecular Bacteriology and Infection, Imperial College London, London, SW7 2AZ, U.K.

[b]Department of Microbiology and Immunobiology, Harvard Medical School, Boston, MA 02115, U.S.A.

[1]Current address: Section of Respiratory Infections, National Heart and Lung Institute, Imperial College London, London, W2 1PG, U.K.

[3]To whom correspondence should be addressed. Email: a.grundling@imperial.ac.uk

Keywords: osmotic stress, TN-seq, Tradis, NaCl, KCl, Sucrose, *S. aureus*, DUF25380, Pbp2

Abstract

Staphylococcus aureus is an opportunistic pathogen that causes a variety of diseases. It presents a problem in hospitals as well as communities partly due to the acquisition of multiple antibiotic resistances, which make infections difficult to treat. *S. aureus* is also a frequent cause of foodborne illnesses due to its ability to produce heat stabile toxins that cause nausea, vomiting and diarrhoea even in the absence of living cells. One contributing factor for the food association is its high salt tolerance, which allows this organism to survive commonly used methods of food preservation. How this resistance is mediated is poorly understood. In this study, we used TN-seq-based high throughput screens to find genes that are involved in the salt tolerance of *S. aureus* and identified the previously uncharacterized DUF2538 domain containing gene *SAUSA300_0957* (gene *957*) as essential under salt stress. Further experiments revealed that a *957* mutant strain is less susceptible to oxacillin and shows increased peptidoglycan crosslinking. The salt sensitivity phenotype could be suppressed by point mutations in the transglycosylase domain of the penicillin binding protein gene *pbp2*, and these mutations also restored the peptidoglycan crosslinking to WT levels. These results indicate that increased crosslinking of the peptidoglycan can be detrimental and highlight the role of the bacterial cell wall for osmotic stress resistance. To gain more information on the general osmotic stress response of *S. aureus* and how responses differ between different osmotic stressors, additional TN-seq studies were performed with KCl and sucrose. Although it is generally assumed that a generic osmotic stress response exists, our results revealed distinctly different long-term responses to NaCl, KCl and sucrose stress. Using a global and genome-wide TN-seq approach, we were able to link numerous previously unknown factors to the osmotic stress response in *S. aureus*. This study will also serve as a starting point for future research in osmotic stress and might help us develop strategies to tackle foodborne staphylococcal infections.

24 **Introduction**

25 *Staphylococcus aureus* is a Gram-positive bacterium that is carried by about 20% of healthy
26 individuals [1]. It is also an opportunistic pathogen causing a variety of diseases, including
27 bacteremia, endocarditis, soft tissue infections and food poisoning [2]. One characteristic of *S.*
28 *aureus* is its ability to grow in the presence of a very high salt concentration up to 2.5 M, conditions
29 under which other bacteria are unable to survive [3], and this has been used extensively for the
30 isolation of staphylococci. This salt tolerance also allows *S. aureus* to thrive in its niches such as the
31 human nares, skin [1] and certain food products [4].

32 In general, the bacterial cytoplasm is hyperosmotic to the environment and can therefore
33 tolerate a certain level of external osmotic stress. However, an increase in the intracellular sodium
34 concentration can lead to mis- and unfolding of proteins and inhibit enzymatic reactions. Hence, *S.*
35 *aureus* must possess strategies to counter the effects of osmotic damage, but these are poorly
36 understood, as most work has been performed in *Escherichia coli* and *Bacillus subtilis*, which possess
37 much lower salt tolerances than Staphylococci.

38 General mechanisms of osmotic stress mitigation are the rapid import of potassium into the cell
39 to reduce the influx of sodium and efflux of water [5-7]. However, during prolonged NaCl stress,
40 potassium levels decrease again after its initial accumulation in the cytoplasm of *S. aureus* [8, 9].
41 Instead, *S. aureus* accumulates small osmotically active compounds, named compatible solutes [3].
42 The most effective compatible solutes in *S. aureus* are glycine betaine and proline [3, 10-14], which
43 are imported by specific osmolyte transporters [13, 14]. These preferred osmolytes can accumulate
44 in the cell to very high concentrations without negatively affecting cellular processes [6]. In addition,
45 *S. aureus* can also synthesize compatible solutes *de novo*, as in the case of glutamine [12], but this
46 process is much slower than the uptake of osmolytes and requires more energy.

47 Consistent with these observations, previous research studying the underlying genetic factors
48 of the *S. aureus* osmotic stress response implicated several osmolyte transporters in this process
49 [15-19]. These include the potassium transport systems Kdp and Ktr [15], the proline transporter
50 PutP [17, 19], the arsenic transport system Ars [16] and the branched chain amino acid uptake
51 system BrnQ [18]. In addition, although currently not experimentally verified, it can be assumed that
52 the main glycine betaine uptake system OpuD [20, 21] is an important factor for osmotic adaptation
53 as glycine betaine uptake reduces sensitivity to NaCl exposure significantly [10].
54 Despite these multiple countermeasures, exposure of *S. aureus* to high salt concentrations also
55 leads to morphological changes, including the formation of larger cells [22] and a thickening of the
56 cell wall [23]. However, if and which genetic factors are required for those processes are currently
57 not well understood. The cell wall of Gram-positive bacteria is an important barrier against osmotic
58 stresses and acts as a counterpart to the pressurized cytoplasm. A major component of the cell wall
59 is peptidoglycan, a polymer consisting of chains of repeating N-acetylglucosamine (GlcNAc) and N-
60 acetylmuramic acid (MurNAc) units that are crosslinked with neighboring chains via short peptides
61 and, in the case of *S. aureus,* pentaglycine cross-bridges (Reviewed by [24]). In the past, the
62 contribution of the cell wall towards osmotic stress resistance was often not considered in the
63 bacterial osmotic stress resistance field, presumably because the integrity of the cell wall was
64 assumed to be a prerequisite rather than an active adaptation to survive osmotic stresses.
65 Nevertheless, several possible changes to the cell wall have been observed *in S. aureus* during NaCl
66 stress, such as shortened interpeptide bridges in the peptidoglycan [22], an increase in resistance
67 to methicillin [25] and increased autolysis activity [26, 27]. In addition to peptidoglycan, other
68 components within the cell envelope, such as teichoic acids and more specifically their modifications
69 with D-alanine [28] and sugar residues [29, 30] are affected by osmotic stress. Combined, these
70 findings indicate that the integrity of the cell wall is an important requirement for osmotic
71 resistance.

72 Most studies on osmotic stress in *S. aureus* have been conducted with NaCl as osmotic stressor.
73 The ionic properties of NaCl have important implications on protein stability and activity as its
74 accumulation can lead to denaturation of proteins. A few studies in *S. aureus* have also been
75 performed with non-ionic osmotic stressors such as sucrose, sorbitol glycerol and amino acids [17,
76 31-33]. These different stresses are often used synonymously with osmotic stress, in part influenced
77 by the findings that the initial mitigation of osmotic stress by either salts or sugars can be prevented
78 by the accumulation of potassium and compatible solutes. However, there are potential differences
79 in the long-term adaptation to ionic and non-ionic osmotic stressors, which have not been
80 investigated in detail up to date. It is currently also not known if adaptations besides the
81 accumulation of potassium and osmolytes are similar or differ depending on the osmotic stressor,
82 and this was addressed as part of this study.
83 Using a transposon insertion sequencing (TN-seq) method [34], we determined on a whole
84 genome level genes that are essential or dispensable during long-term osmotic stress caused by the
85 exposure to NaCl. Several unknown and understudied genes were identified as essential under salt
86 stress including *SAUSA300_0957,* coding for a cytoplasmic protein, which we show here is important
87 for peptidoglycan homeostasis in *S. aureus*. Another protein, which we identified as important
88 during salt stress and essential for peptidoglycan synthesis, is the penicillin binding protein Pbp2,
89 again highlighting a key function of peptidoglycan during NaCl-induced salt stress. To determine
90 how the response varies depending on the osmolyte used, TN-seq screens were also performed in
91 the presence of KCl and sucrose. This yielded very different sets of essential and dispensable
92 candidate genes, providing experimental evidence of the distinct nature of these stresses and linking
93 a number of previously unknown factors to the osmotic stress response in *S. aureus*.
94

95 **Results**

96 **TN-seq analysis identifies *S. aureus* genes involved in NaCl stress**

97 To identify genes involved in the *S. aureus* salt stress response, two independent transposon
98 sequencing (TN-seq) screens were conducted at different salt concentrations and generation times
99 (Figure 1A). A multiplexed transposon library, generated using 6 different transposons possessing
100 different or no promoters [34, 35], was used in replicate A and an independent Tn-library using a
101 transposon without an outward facing promoter was used in replicate B. In both experiments, LB
102 medium with either the normal salt concentration of 85 mM NaCl (LBN), LB medium with extra
103 0.25M NaCl or LB medium with extra 0.5 M NaCl was used (See Supplementary Table S1 for a list of
104 all TN-seq experiments). Monitoring bacterial growth over seventeen generations, revealed that
105 growth in LB 0.25M NaCl was comparable to that of cells grown in LBN (Figure 1B), whereas a strong
106 reduction in growth was seen in the presence of 0.5M NaCl (Figure 1B). For the TN-seq analysis,
107 samples were taken after 10 and 17 doublings. As expected, the Tn insertions were distributed
108 evenly throughout the genome when the bacteria were propagated in LBN but became more
109 unbalanced at higher salt concentrations and longer generation times due to the enrichment of
110 better salt-adapted TN-strains (Supplementary Figure 1). The fold-change of transposon insertions
111 per gene under the salt stress conditions compared to the LBN condition (input library) as well as q-
112 values (false discovery rate according to Benjamini-Hochberg) were determined for each gene
113 (Supplementary Table S2 & 3). The data were also plotted as volcano plots (Figure 1C), in which
114 negative values on the x-axis indicate genes that are essential under high salt conditions (fewer TN
115 insertions in high salt), whereas positive values indicate dispensable genes, for which an inactivation
116 might be beneficial under high salt conditions. For replicate A, after 10 generations in the presence
117 of 0.25M NaCl the number of TN insertions per gene was not drastically altered compared to LBN
118 (Figure 1C, top row). An increase in the salt concentration with the same number of generations

119 slightly increased the number of essential and dispensable genes, but the number was still quite low
120 (Figure 1C, top row). Extending the growth to 17 generations (Figure 1C, second row) increased the
121 number of genes with significant differences in the number of TN-insertions during growth at 0.25
122 M NaCl and even more so at 0.5 M NaCl, indicating a much more stringent depletion or enrichment
123 of strains with TN-insertions in specific genes from the input library. Therefore, the TN-seq
124 experiment for replicate B was only performed with 17 generation samples (Figure 1C, bottom row;
125 Supplementary Table 3). Lists of the top common shared genes between conditions were created
126 (Supplementary Tables S4-7) and the reproducibility between experiments was also assessed by a
127 principal component analysis (PCA) (Figure 1D). For the 17 generation data sets, a clear difference
128 between cells grown in either 0.25 M (orange ellipse) or 0.5 M NaCl (red ellipse) was observable and
129 experimental data points clustered together for each condition. The 0.25 and 0.5 M NaCl data from
130 the 10 generation experiment, which was only conducted once, clustered both closely with the 17
131 generation 0.25 M NaCl samples, consistent with considerably fewer changes in depleted or
132 enriched TN-strains under these conditions as compared to growth for 17 generations in LB 0.5 M
133 NaCl. From this analysis we concluded that growing *S. aureus* for 17 generations in 0.5 M NaCl
134 medium provides sufficiently stringent conditions to identify genes that are either essential or
135 dispensable in high salt conditions and our further analysis focused on these data sets.
136

137 **The TN-seq screens highlight the essentiality of transporter and cell envelope related genes and**
138 **the dispensability of respiration genes under high salt conditions**

139 To provide a visual and genome wide guide to the cellular functions of salt essential or dispensable
140 genes, Voronoi maps were generated for the 17 generation 0.5 M NaCl datasets [36, 37]. For this
141 global visualization, the observed decrease (essential genes) or increase (dispensable genes) in Tn
142 insertions per gene compared to LBN medium were plotted regardless of their p-value

143 (Supplementary Figures 2 and 3). In both replicates, genes coding for transporters and cell envelope
144 related genes were the most prominent conditionally salt essential genes (Supplementary Figure 2).
145 More specifically, the TN-Seq data indicated that inactivation of the putative magnesium
146 transporter MgtE [38] and the putative D-serine/D-alanine/glycine transporter AapA is detrimental
147 under salt stress. Inactivation of AapA has previously been shown to suppress the temperature
148 sensitivity phenotype seen in an *S. aureus fmtC/mprF* mutant [39] and to lead to increased
149 amoxacillin and daptomycin sensitivity [35, 40]. In addition, the *dlt* operon, coding for enzymes
150 required for the D-alanylation of teichoic acids, an important factor for cationic peptide resistance
151 [41], as well as the stationary and stress sigma factor gene *sigB* were found to be essential.
152 An even larger number of genes was identified as dispensable during salt stress (Supplementary
153 Figure 3). Inactivating or reducing the expression of such genes is expected to help *S. aureus* survive
154 under salt stress. Among these dispensable genes were genes coding for the sodium antiporter
155 Mnh2, which has previously been shown to transport Na^+/H^+ and K^+/H^+ in high pH medium and to
156 play an important role in cytoplasmic pH maintenance [42]. Strikingly, a large number of genes
157 involved in respiration, such as the *cta/qox/men/hem* operons as well as genes involved indirectly
158 in respiration through quinone synthesis (shikimate pathway, *aro* operon) were also identified as
159 dispensable during salt stress. Curiously, the data also reproducibly indicated that genes coding for
160 the phosphodiesterases GdpP and Pde2 involved in degradation of the signaling molecule c-di-AMP
161 are dispensable under high salt conditions. Somewhat contradictory, the construction of a *dacA*
162 mutant coding for the cognate c-di-AMP cyclase DacA was only possible at high salt concentrations
163 (or in defined chemical medium) [21]; but altogether these findings confirm the involvement of c-
164 di-AMP in salt mediated osmotic stress adaption in *S. aureus*.

165 **Confirmation of genes essential during salt stress using individual mutants**

166 To determine to what extent different genes identified in the TN-seq screen contribute to the salt
167 resistance of *S. aureus*, a set of candidate genes from the top hits of the 17 generations, 0.5 M NaCl
168 LB dataset B were chosen for further analysis. For this analysis we used defined transposon mutants
169 available from the *S. aureus* NTML transposon mutant library [43] (Supplementary Table S8). Most
170 of the chosen genes showed similar trends in dataset A, but intriguingly two of the tested genes,
171 *rsbV* and *rsbW*, were flagged as highly dispensable in dataset A but as essential in dataset B. Since
172 no strains with transposon insertions in the *dlt* operon were available in the NTLM transposon
173 mutant library the contribution of these genes to the salt stress resistance was not further
174 investigated.

175 Next, the growth of the different NTML transposon mutant strains was assessed in LBN and LB 0.5
176 M NaCl medium. In LBN medium, most strains grew similarly to the WT strain JE2, indicating that
177 inactivation of the respective gene does not greatly affect bacterial growth in normal LB medium
178 (Figures 2A-D, left panels). Exceptions were strains NE1109 (*sigB*) (Figure 2A), NE1778 (*lcpB*) (Figure
179 2B) and NE188 (*mfd*) (Figure 2C), cultures of which reached slightly lower final optical densities. At
180 high osmolarity conditions (LB 0.5 M NaCl), all strains showed a growth defect compared to the WT
181 strain (Figures 2A-D), validating TN-seq as a method to identify genes important in *S. aureus* during
182 salt stress. Several strains exhibited strong growth defects in the presence of 0.5 M NaCl (Figures 2C
183 and D) with strain NE1384 (*SAUSA300_0957*) showing extremely reduced growth (Figure 2D). To
184 confirm that the salt sensitivity was mediated by the inactivation of the genes in questions, we
185 constructed complementation plasmids for seven of the most promising candidates by either
186 expressing the gene of interest from its native promoter or an anhydrotetracycline (Atet) inducible
187 promoter in the transposon mutant strains. While no complementation was observed for four
188 strains (Supplementary Figures 4A and B), the salt-dependent growth defect could be
189 complemented for strains carrying mutations in *SAUSA300_0694* (Figure 3A), *SAUSA300_0910*

190 (*mgtE*) and *SAUSA300_0957* (Figure 3B). *SAUSA300_0694* encodes a hypothetical protein with 6
191 predicted transmembrane helices but no other identifiable domain motif. MgtE (SAUSA300_0910)
192 is a predicted magnesium transporter. *SAUSA300_0957* (from here on also referred to as gene *957*)
193 codes for a cytoplasmic protein of unknown function and was further investigated in this study
194 because a *957* mutant exhibited the strongest salt-sensitivity phenotype.

195 **Genomic organization of *957* suggests a potential function in cell envelope homeostasis**

196 *SAUSA300_0957* encodes a protein with a DUF2538 domain of unknown function. Proteins with this
197 domain are found mainly in Gram-positive bacteria (Actinobacteria and Firmicutes) (based on an
198 Interpro search, https://www.ebi.ac.uk/interpro/entry/IPR024469). Although a crystal structure of
199 the 957 protein has been deposited in the PDB (3KBY), to our knowledge nothing is known about
200 the actual cellular function of this protein. Transcriptome data [44] suggest that gene *957* is in an
201 operon with *lcpB* (Figure 4A). LcpB is one of three wall teichoic acid (WTA) ligases present in *S.*
202 *aureus* that attaches WTA to the peptidoglycan polymer [45-47]. Inactivation of LcpB leads to slightly
203 lower WTA levels in the cell wall, whereas deletion of all three WT ligases completely abolishes WTA
204 anchoring to the cell wall [45]. In addition, LcpB cell wall ligase activity was demonstrated *in vitro*
205 [47]. *fmtA* is located upstream of the *957* operon and has been proposed to code for an esterase
206 that can remove D-alanine modifications from teichoic acids [48] and is involved in methicillin
207 resistance [49]. Genes coding for a predicted acetyltransferase and *atl* coding for the major *S. aureus*
208 autolysin are found immediately downstream of the *957* operon [50]. In this early work, gene *957*
209 was first described as an ORF of "unknown function". Since functionally related genes often cluster
210 together in bacteria, this prompted us to next look at cell-envelope related phenotypes for a *957*
211 deletion strain.

212 **Deletion of gene *957* causes physiological changes leading to a smaller cell size**

213 As all previous experiments were performed with transposon mutants, we first constructed strain
214 LAC*Δ*957* with a marker-less in-frame deletion of gene *957*. Strain LAC*Δ*957* had the expected
215 growth defect in the presence of 0.5 M NaCl, which could be complemented by expressing a
216 functional copy of *957* (Figure 4B). We then proceeded to test if the *957* mutant displays other
217 phenotypes and to investigate if gene *957* is involved in cell envelope homeostasis. First, WT LAC*,
218 the *957* mutant and the complementation strain were grown in LBN and the ratio of colony forming
219 units to optical density (CDU/OD) was determined. The CFU/OD ratio was significantly larger for the
220 *957* mutant (60.8±6.8 x10^7 CFU/OD) mutant as compared to strain LAC* (37.5±9.3 x10^7 CFU/OD)
221 when grown in LBN, suggesting a change in cell shape or size (Figure 4C). This phenotype was
222 restored in the complementation strain (37.3±3.6 x10^7 CFU/OD) (Figure 4C). When the average cell
223 diameter was determined by microscopy, a small but significant reduction in cell diameter was seen
224 for the *957* mutant (1.25±0.02 µm) as compared to the WT (1.36±0.03 µm) and the cell size was
225 restored to wild type levels in the complementation strain (1.35±0.05 nm) (Figure 4D).

226 **Salt sensitivity of *957* is not due to interaction with LcpB but likely due to changes in peptidoglycan**
227 **crosslinking**

228 Since the gene *957* is on the same transcript as *lcpB* coding for a WTA ligase (Figure 4A), the
229 contribution of WTA to salt stress resistance as well as the contribution of *957* to the attachment of
230 WTA to the cell wall was assessed. Initially the growth of a *tagO* (*tarO/llm*) mutant, a strain unable
231 to produce WTA, was tested in LB and LB 0.5 M NaCl medium. When cells were grown in LBN, they
232 grew normally (Supplementary Figure 5A), but under high salt conditions, the *tagO* mutant showed
233 reduced growth, similar to that of the *957* mutant (Figure 5A). This is consistent with what has been
234 reported previously for a *Staphylococcus epidermidis tagO* mutant [51] and indicates an important

235 role for WTA during salt stress. When the *lcpB* mutant was propagated in LBN medium, its growth
236 was slightly inhibited (Supplementary Figure 5A). However, in high salt medium (Figure 5A) it grew
237 unimpeded and like WT. Since the *lcpB* mutant did not show a growth defect in high salt medium,
238 this made it unlikely that *957* is a regulator of LcpB activity. To further exclude that gene *957* could
239 be somehow involved in the attachment of WTA to the peptidoglycan, we isolated WTA from strains
240 grown in either LB or LB containing 0.4 M NaCl and separated the polymer on native polyacrylamide
241 gels. The slightly lower concentration of salt was chosen because growth of the *957* and the *tagO*
242 mutants was too strongly inhibited at 0.5 M NaCl. As expected the *tagO* mutant did not produce
243 any WTA (Supplementary Figure 5B, Figure 5B) and consistent with previous studies [45, 46], the
244 *lcpB* mutant exhibited slightly reduced WTA levels compared to all other strains (Supplementary
245 Figure 5B, Figure 5B). There was no reduction of WTA observable in the *957* mutant compared to
246 the WT strain in either LBN (Supplementary Figure 5B & 5C) or LB 0.4 M NaCl (Figure 5B & 5C) but
247 rather a small, complementable increase, suggesting no influence of *957* over LcpB on WTA
248 attachment.
249 Gene *957* is found upstream of the bi-functional autolysin gene *atl* and therefore we next
250 investigated potential changes in autolytic activity using zymograms. Cell extracts from overnight
251 cultures of the WT, the *957* mutant and the complementation strain were separated on
252 polyacrylamide gels with embedded *Micrococcus luteus* cells and incubated overnight in buffer to
253 re-fold the autolysins and enable the digestion of the peptidoglycan. A small increase in autolytic
254 activity was detected in the *957* mutant (Figure 5D) for bands around 55 kDa and 70 kDa compared
255 to the WT and complementation strain, indicating a possible change in Atl availability. We also
256 tested the susceptibility of the *957* mutant towards the cell wall active beta-lactam antibiotic
257 oxacillin. In contrast to our expectations, the *957* mutant exhibited a small but significant increase
258 in MIC towards this antibiotic than the WT or the complementation strain (Figure 5E), indicating
259 potential changes to the peptidoglycan structure. To test this, we next analyzed the muropeptide

260 profile of mutanolysin-digested peptidoglycan isolated from the WT, the *957* mutant and
261 complementation strain after growth in LBN or LB 0.4 M NaCl medium. Upon first inspection, no
262 peaks were absent in any condition or strain (Supplementary Figure 5D, Supplementary Figure 5E).
263 Probing further, mono- and multimers of muropeptides up to 7-mers (see Supplementary Figure 5D
264 for how binning was performed) were quantified but no significant changes were found when
265 strains were cultured in LBN medium (Supplementary Figure 5F). However, when the muropeptide
266 profiles from cells cultured in 0.4 M NaCl were compared, a significant decrease in the total amount
267 of di- and trimers and a significant increase in higher multimers was observed for the peptidoglycan
268 isolated from the *957* mutant (Figure 5F), suggesting that sensitivity to NaCl could potentially be
269 caused by higher crosslinking and rigidity of the peptidoglycan in the mutant.

270 **Salt-resistant suppressors possess variations in the transglycosylase domain of Pbp2 and show**
271 **reduced peptidoglycan crosslinking**

272 Next, we attempted to generate *957* suppressor strains that showed improved growth in the
273 presence of 0.5 M NaCl, with the idea that by mapping and investigating the compensatory
274 mutations, further insight into the cellular functions of protein 957 could be gained. We initially
275 attempted to raise suppressor strains on solid medium but failed to do so, because the growth
276 defect of the *957* mutant was not as prevalent on agar plates. We therefore used liquid medium
277 instead, where we readily obtained suppressor strains. These strains grew as well as or even better
278 than the WT LAC* strain in the high salt conditions (Figure 6A) and also grew similar to the WT in
279 LBN (Supplementary Figure 6A). The genome sequences of 10 independent suppressor strains were
280 determined and single nucleotide polymorphisms (SNPs) in one or two genes could be identified for
281 each strain (Supplementary table S9), except for one strain where the coverage was insufficient, and
282 this strain was omitted from further analysis. A common denominator for all suppressor strains were
283 SNPs in the *pbp2* gene, coding for the Penicillin binding protein 2 (Pbp2) (Figure 6B). *S. aureus* Pbp2

284 is a bifunctional enzyme [52, 53], which possesses transglycosylase and transpeptidase activity and
285 is involved in peptidoglycan synthesis. All nine discovered SNPs were unique and led to mutations
286 in the amino acid sequence in the transglycosylase domain but neither to stop codons, nor
287 frameshifts nor mutations in the transpeptidase domain. The mutations were mapped (Figure 6B)
288 onto an available Pbp2 structure (3DWK) [54] to see if a specific area of the transglycosylase domain
289 had been targeted, but the amino acid substitutions were found throughout the molecule and not
290 only in the active site. Interestingly, *pbp2* also appeared to be considerably less important for
291 growth at 0.5 M NaCl (Supplementary Figure 6B and 6C), although transposons were mainly
292 localized at the beginning and end of the gene or within the promoter region.
293 To confirm that the *pbp2* SNPs were indeed responsible for the suppression of the salt sensitivity of
294 the *957* mutant, we transferred the *pbp2* SNPs from two strains into a fresh LAC*Δ*957* background
295 by co-transduction of a transposon in a nearby gene (Supplementary Figure 6D, schematic). As
296 expected, these "recreated" suppressor strains showed also increased salt resistance (Figure 6C,
297 Supplementary Figure 7A). In addition, we repaired the *pbp2* gene in two suppressors to the WT
298 *pbp2* allele and this reduced their ability to cope with NaCl stress, all consistent with the hypothesis
299 that the SNPs in *pbp2* are responsible for the suppression phenotype (Figure 6D, Supplementary
300 Figure 7B). When the same *pbp2* SNPs were transferred into a WT LAC* strain, a reproducible
301 growth improvement of the SNP-bearing strains was observed in high salt medium, an indication
302 that the *pbp2* mutations lead to a general growth improvement of *S. aureus* under NaCl stress
303 conditions (Figure 6E, Supplementary Figure 7C).
304 Moenomycin is a phosphoglycolipid antibiotic that inhibits the transglycosylase activity of the *S.*
305 *aureus* Pbp2 enzyme (reviewed in [55]). To test if a decrease in Pbp2 transglycosylase activity results
306 in the improved growth of the *957* mutant in high salt conditions, cells were grown on LB agar
307 containing 0.5 M NaCl with or without moenomycin. The growth behaviors of the WT strain and the
308 *957* mutant were similar when grown on solid LB agar containing 0.5 M NaCl but lacking

309 moenomycin (Figure 6F, top panel). As stated above, this discrepancy in the growth behavior of the
310 *957* mutant in high salt liquid versus solid medium was already noted when we attempted to
311 generate suppressors on agar plates. On the other hand, in medium supplemented with 0.02 µg/ml
312 moenomycin, we observed better growth of the *957* mutant compared to the WT strain (Figure 6F,
313 lower panel). In addition, the *957* mutant also showed improved growth compared to the two
314 suppressor strains S2 and S4 when moenomycin was added (Figure 6F, lower panel). These findings
315 are consistant with the idea that a partial inhibition of the glycosyltransferase activity of Pbp2 can
316 improve the growth of the *957* mutant in high salt medium.

317 Because the LAC*Δ*957* strain showed increased peptidoglycan crosslinking when compared
318 to a WT strain, we hypothesized that the peptidoglycan of the suppressor strains would be again
319 less crosslinked. To test this, the peptidoglycan from two of the suppressor strains grown in LB 0.4
320 M NaCl was isolated, the muropeptide profiles determined and compared to that of the original *957*
321 mutant (Figure 6G, Supplementary Figure 7D). As before, the muropeptide profiles looked similar
322 (Supplementary Figure 7D) but quantification revealed a significant reduction in crosslinked
323 peptidoglycan fragments and a significantly overrepresentation of monomeric and dimeric
324 fragments in the suppressor strains as compared to the original *957* mutant (Figure 6G). These
325 results indicate that the amount of crosslinking of the peptidoglycan polymer is an important factor
326 in the salt resistance of *S. aureus* and that dysregulation of peptidoglycan crosslinking can lead to
327 destabilizing effects.

328 **Different types of osmotic stresses target different sets of genes**

329 In the literature, osmotic stress is a loosely used term for any accumulation of osmolytes, however
330 the type of ion or osmolyte can potentially have a great impact how bacteria respond. To address
331 this issue, we then determined how the stress response between different commonly used
332 osmolytes compare. To this end, the highly saturated *S. aureus* transposon library with the

333 promoter-less transposon was propagated for 16 generations while challenged with either 0.5 M
334 NaCl, 0.5 M KCl or 1.0 M sucrose (Figure 7A). The molarity for sucrose was doubled, as the salts
335 dissociate into two molecules whereas the sucrose does not. The culture challenged with 0.5 M NaCl
336 grew the slowest, followed by 1.0 M sucrose, whereas the cells grown in 0.5 M KCl grew similarly to
337 the cells grown in LBN (Figure 7B). Of note, the optical density measurements of *S. aureus* in 1.0 M
338 sucrose proved to be difficult because the OD_{600} values dropped dramatically upon diluting cells into
339 this medium. In all likelihood, the exposure leads to shrinking of the cells and therefore reduced
340 absorbance, resulting in values too low to detect in the first two hours.
341 As expected by using a large and good quality transposon library, transposon insertions were found
342 under all conditions in genes throughout the whole genome (Figure 7C). Next, the number of TN-
343 insertions per gene following growth under the NaCl, KCl or sucrose stress condition was compared
344 to the number of TN-insertions per gene after growth in LBN medium (Supplementary table S10)
345 and in this manner conditionally essential (Supplementary table S11) and dispensable
346 (Supplementary table S12) genes identified. Fold-changes in transposon insertions per gene and q-
347 values were plotted in volcano plots (Figure 7D). From this, it was evident that under KCl stress the
348 number of essential and dispensable genes was much lower than for NaCl or sucrose stress,
349 indicating a much less severe effect of KCl on *S. aureus* cells. Sucrose stress also showed a reduced
350 set of essential and dispensable genes compared to NaCl stress, but considerably higher than under
351 the KCl condition. This was also reflected when inspecting the gene lists of the top 30 essential or
352 dispensable genes (Supplementary table S11-12) as in the KCl condition only 15 and 2 genes
353 respectively met the requirements of q-value ≤ 0.05 and a fold-change of 5. To identify common
354 genes between conditions, the fold-change stringency was relaxed to 2-fold and the overlap of
355 genes was visualized in Venn diagrams (Figure 7E, individual genes in Supplementary Table S13).
356 Three genes, namely *SAUSA300_0425* (*USA300HOU_0457*, *mpsA (nuoF)*, a cation transporter of the
357 respiratory chain [56]) *SAUSA300*_0750 (*USA300HOU_0796*, *whiA*, a hypothetical protein, possibly

358 involved in cell wall synthesis) and SAUSA300_0846 (USA300HOU_0903, a possible sodium:proton
359 antiporter) were essential in all conditions. In the case of dispensable genes, only one gene,
360 *SAUSA300_1255* (*USA300HOU_1294*, *mprF/fmtC*), coding for a phosphatidylglycerol
361 lysyltransferase involved in the defense against cationic microbial peptides, was identified in all
362 conditions (Figure 7E, (Supplementary Table S12). Overall, the overlaps between conditions were
363 small, indicating distinct modes of actions for each osmotic stress.
364 Next, in order to assess similarities and differences on a gene function and cellular pathway level,
365 functional Voronoi maps were generated from the conditionally essential (Figure 8) and dispensable
366 (Supplementary Figure 8) genes regardless of their p-values. These images highlighted the
367 essentiality of the wall teichoic acid through *tagO* and the *dlt* operon (Figure 8A) as reported in the
368 first two experiments for the 0.5 M NaCl condition and the essentiality of the transporters AapA and
369 MgtE in both NaCl (Figure 8A) and KCl (Figure 8B) stress conditions. In the high sucrose condition,
370 these transporters were much less prominent (Figure 8C). The patterns of essential genes suggested
371 a similar stress response for the ionic stressors NaCl and KCl that was distinct from sucrose stress.
372 When the dispensable genes were investigated (Supplementary Figure 8), the number and type of
373 genes in the NaCl condition differed considerably from KCl and sucrose stress. Under NaCl stress
374 (Supplementary Figure 8A), in addition to the penicillin binding protein *pbp2*, a large number of
375 genes involved either directly in respiration or indirectly by their role in ubiquinone synthesis were
376 found to be dispensable (Supplementary Figures 3A, 3B and 8A). The number of dispensable genes
377 in the KCl (Supplementary Figure 8B) and sucrose (Supplementary Figure 8C) conditions were
378 considerably less, indicating differences in the osmotic stress response between NaCl and KCl.

379 **Verification of KCl sensitivity of conditionally essential genes identified by TN-seq**

380 Next, from the pool of genes postulated to be essential under KCl stress, and also taking into account
381 genes that overlapped between NaCl and KCl conditions (Figure 8A and B), mutants were selected

382 for growth analysis in medium containing 0.5 M KCl. This included strains NE736 (*SAUSA300_0910*,
383 *mgtE*), NE867 (*SAUSA300_0483*, *mazG*) and NE810 (*SAUSA300_1642*, *aapA*) (Figure 9). In addition,
384 NE1384 (SAUSA300_0957, *gene 957*) was also included. When grown in LB medium supplemented
385 with 0.5 M KCl, all strains showed a strong growth defect compared to the WT strain JE2 (Figure 9A,
386 LBN curves in Figure 2). The strongest growth defect was observed for the *mgtE* mutant strain
387 NE736. This is in line with our TN-seq data, as the *mgtE* gene was identified as the top candidate of
388 essential genes in the KCl condition (Supplementary table S11). MgtE is a putative
389 magnesium/cobalt transporter with a cystathionine-beta-synthase (CBS) domain that is thought to
390 regulate ion translocation [57] but not much is known in *S. aureus*. In previous studies, we
391 determined that the CBS domain of MgtE is not a c-di-AMP target [58] and we recently
392 demonstrated that MgtE is an important contributor to cobalt toxicity in *S. aureus* [38]. To verify the
393 KCl sensitivity, growth curves were repeated with a clean Δ*mgtE* mutant and complementation
394 strain. In LBN medium a slight, but complementable, growth defect was detectable for the *mgtE*
395 mutant but an almost complete growth arrest was seen in LB medium supplemented with 0.5 M KCl
396 (Figure 9B). Taken together, we present robust data on different osmotic stresses and our results
397 indicate that the osmotic stresses caused by NaCl, KCl and sucrose are distinct from each other.
398 Nevertheless, some genes such as *mgtE* play an important role in more than one condition and are
399 therefore valuable targets for upcoming studies.

400 **Discussion**

401 In this work, we successfully identified several salt tolerance genes in the USA300 *S. aureus* strain
402 and further characterized gene *957,* a gene without previously assigned function. Our results
403 indicate that the gene product is involved in cell envelope homeostasis but likely not WTA
404 attachment and we show that its absence leads to more crosslinked peptidoglycan. Suppressors of
405 a *957* mutant acquired mutations in *pbp2* and the increase in peptidoglycan crosslinking was
406 reversed in such stains. This demonstrates that the synthesis of the peptidoglycan layer is a tightly
407 regulated process that plays an essential role during osmotic stress. In addition, we tested other
408 osmotic stresses and performed TN-seq screens and could show that each osmotic stressor affects
409 a defined but different set of genes. It is therefore important to use the term osmotic stress
410 carefully, as our results highlight that there is not a general osmotic stress response but rather
411 responses tailored to the individual osmolyte.

412 TN-seq experiments provide a wealth of information about the growth ability of single mutants in a
413 mixed population and can therefore quickly and accurately determine genes that are required under
414 certain growth condition. It is however always a concern that a single TN-seq experiment might not
415 be reproducible due to stochastic extinction of individual mutants or certain growth dynamics. In
416 this study, we performed three independent NaCl TN-seq experiments using two different libraries
417 and slightly different experimental setups. Although there were differences between experiments,
418 overall the data (0.5 M NaCl LB, 17 generations) proved to be rather consistent between different
419 runs (Figure 1D) suggesting that a single experiment would be sufficient in most cases.

420 Because TN-seq relies on the selection of strains adapted to certain growth conditions, competition
421 between mutants and subsequent depletion of the input library it is to be expected that this method
422 is ideal for exploring the long-term effects on growth instead of quick, short-term response to
423 stresses. To evaluate how our TN-seq results compared to previous results from high-throughput

424 studies of *S. aureus* cells grown in high salt conditions, we determined the overlaps between our 0.5
425 M NaCl, 17 generation datasets and a microarray data set acquired from cells grown for ~6
426 generations in 2 M NaCl [15]. To compare the datasets, the *S. aureus* strain COL locus tags used in
427 the microarray study were first converted to TCH1516 locus tags where possible (Supplementary
428 Table S14) and afterwards compared with the first two 0.5 M NaCl, 17 generation TN-seq datasets.
429 The overlap between the downregulated (microarray) and dispensable (TN-seq) genes was minimal
430 in both replicates (1 and 7) and also very small for the upregulated and essential genes (both 14).
431 Three operons were consistently essential or upregulated between all datasets: the *cap5*,
432 *SAUSA300_0771-2*, and the *sda* operon. The *cap5* genes are involved in capsule production [59] and
433 this type of capsule has been previously reported to be induced by the addition of salt [60]. Genes
434 *SAUSA300_0771-2* are hypothetical membrane proteins and presumably part of a threonine/serine
435 exporter (Interpro database IDs: IPR010619 and IPR024528) and the *sda* genes are annotated as L-
436 serine dehydratase components and a regulator protein. Taken together, the low overlap between
437 the microarray and TN-seq data (Supplementary Table S14) further highlights that in our screen we
438 have identified a number of previously unknown salt tolerance genes.
439 Most mutants of potential NaCl essential genes identified in the TN-seq screen proved to be
440 sensitive to 0.5 M NaCl (Figure 2A-D), confirming the effectiveness of the TN-seq screen. In
441 particular, previously uncharacterized genes such as *SAUSA300_0694*, *mgtE,* and the *957* gene could
442 be identified as essential during NaCl stress and their phenotypes could be complemented (Figure
443 3). In our study, we opted not to experimentally validate any of the dispensable genes, as the
444 verification of a growth advantage is more difficult to prove than a growth defect, but these genes
445 will provide interesting starting points for future research. In addition, it will be interesting to
446 investigate higher concentrations of NaCl to see if the same or different genes are flagged as
447 essential and dispensable.

448 Gene *957* was selected for further characterization as part of this study, because it had previously
449 not been linked to NaCl stress and had not been investigated before. As gene *957* and *lcpB* are co-
450 transcribed we initially assumed that protein 957 is involved in WTA attachment via LcpB but we
451 were unable to demonstrate such a link. Instead the *957* mutant exhibited increased muropeptide
452 crosslinking, which could be suppressed by certain *pbp2* SNPs suggesting involvement in
453 peptidoglycan synthesis. We can only speculate if the SNPs identified in *pbp2* increase or inhibit the
454 activity of Pbp2. However, judging by the number of independent SNPs, it seems more likely that
455 the mutations lead to a decrease rather than an increase in transglycosylase activity. In addition,
456 the results from the moenomycin sensitivity experiments using a sublethal antibiotic concentration
457 (Figure 6F) highlights that partial inactivation of the transglycosylase activity of Pbp2 improves the
458 growth of the *957* strain in high salt conditions. This is consistent with the idea that the obtained
459 *pbp2* SNPs lead to a decrease in transglycolylase activity. The absence of frameshift or non-sense
460 mutations can be explained by the importance of the C-terminal transpeptidase domain of *pbp2*
461 [61] and this is reflected in the transposon insertion distributions (Supplementary Figure 6B & C).
462 Intriguingly, the suppressor mutants show reduced growth compared to the *957* mutant on
463 moenomycin plates, presumably due to transglycosylation activity reduced to levels that are
464 detrimental to the cell. At this point it is also unclear how mutations in the transglycosylase domain
465 alter the muropeptide pattern, since the peptide bonds are made by the transpeptidase, not the
466 transglycosylase domain. We hypothesize that a decrease in the efficiency of the glycosylation
467 activity and slowing down the glycan chain synthesis process, will allow reduce the efficiency of the
468 subsequent transpeptidation process, resulting in decreased peptidoglycan crosslinking in the *pbp2*
469 SNP strains. It is also noteworthy that the *pbp2* gene becomes dispensable under NaCl conditions
470 (Supplementary Figure 8A), an additional indicator that Pbp2 activity needs to be avoided under
471 high salt conditions.

472 Interestingly, the *957* mutant exhibited a slightly higher oxacillin MIC than the WT. This is in contrast
473 to what we expected as MICs are determined in 2% (0.342 M) salt medium and this should lead to
474 a growth disadvantage of the mutant. However, when seen in light of the increase in peptidoglycan
475 crosslinking, this could explain the growth advantage of the *957* mutant in the presence of this beta-
476 lactam antibiotic, as this could counter the inhibition of transpeptidases by oxacillin.
477 Although we were unable to determine the exact molecular mechanism, it is clear from our data
478 that gene *957* is involved in cell wall synthesis either directly or indirectly. More generally, our work
479 suggests that the rigidity of the peptidoglycan cell wall is an important factor to counter osmotic
480 stresses and it is conceivable that the more crosslinked cell wall of the *957* mutant is less elastic and
481 therefore easier to break under strong osmotic stress caused by NaCl exposure (Summarized in
482 Figure 10).
483 From our TN-seq data and the use of different osmotic stressors (NaCl, KCl and sucrose), it is evident
484 that although all these compounds exert osmotic stress, the response differs greatly between them
485 (Figure 7, Figure 8 and Supplementary Figure 8). NaCl and KCl conditions share a set of genes that
486 become essential such as the transporters *aapA* and *mgtE* (Figure 8A and B) but differ in the set of
487 dispensable genes (Supplementary Figure 8A and B). It is intriguing that a whole set of respiration
488 related genes become dispensable under NaCl stress but not under KCl stress. This could indicate
489 that respiration should be inhibited or slowed down in high NaCl conditions, possibly by interference
490 with sodium pumps a process less likely to be inhibited by potassium ions. The set of essential genes
491 under sucrose conditions (Figure 8C) was vastly different from that of the NaCl and KCl conditions
492 whereas the set of sucrose dispensable genes (Supplementary Figure 8C) looked similar to the KCl
493 set. This highlights the differences in osmotic stress adaptations and serves as a reminder that the
494 type of stressor remains important. Therefore, although the term osmotic pressure is useful in some
495 contexts, it often needs to be taken with a grain of salt.

496 Using our TN-seq approach, we were able to identify another important factor, the predicted
497 magnesium transporter MgtE, as essential during KCl, as well as NaCl stress. From experiments
498 performed in *E. coli*, it can be inferred that MgtE transports Mg^{2+} ions from the outside of the cell
499 into the cytoplasm [57]. In our previous work, we have shown that the addition of Co^{2+} to the growth
500 medium of a MgtE-carrying *S. aureus* strain leads to a growth defect that can be rescued by deletion
501 of *mgtE* [38], which is in line with cation import by MgtE. Using *in vitro* assays, it was shown for the
502 *E. coli* MgtE transporter that the addition of K^+ or Na^+ does not inhibit Mg^{2+} transport, which means
503 that MgtE is unable to import sodium or potassium. This raises the question why NaCl or KCl would
504 inhibit the growth of an *mgtE* mutant. It is possible that an abundance of KCl or NaCl in the growth
505 medium leads to an increase in these ions in the cell envelope. This could displace magnesium ions,
506 which are an important factor for the stability of the cell wall and a higher requirement of
507 magnesium under NaCl stress has been demonstrated [62]. Deletion of *mgtE* presumably reduces
508 the uptake of magnesium and could reduce magnesium levels in the cell envelope leading to a
509 destabilization of the cell.
510 In conclusion, we have identified a number of previously uncharacterized factors involved in the
511 osmotic stress response of *S. aureus,* which in particular highlighted the importance of the cell
512 envelope and the data generated will provide a great resource for further studies of the
513 staphylococcal osmotic stress response.

514 **Acknowledgements**

515 This research was funded by the Wellcome Trust through grants 100289 and 210671/Z/18/Z to A.G.
516 and the NIH grant P01AI083214 to S.W.. C.F.S. is funded by the German Research Foundation
517 [Deutsche Forschungsgemeinschaft (DFG)] through grant SCHU 3159/1–1 and F.C.M.K. was
518 supported by a Wellcome trust Ph.D. studentship. We thank Microbes NG and the London Institute
519 of Medical Sciences for providing whole genome sequencing services and the Tufts sequencing

520 facility for the sequencing services for the TN-seq experiments. We also would like to thank Ute
521 Bertsche for kind advice on HPLC analyses.

522 **Author contributions**

523 C.F.S., D.M.W., F.C.K. and A.G. performed the research; C.F.S., D.M.W., F.C.M.K., M.S., S.W. and A.G.
524 analyzed the data; C.F.S. and A.G. designed the research; C.F.S. and A.G. wrote the paper. All authors
525 approved the final version of the manuscript.

526 **Conflict of interests**

527 The authors declare not conflict of interest.

528 **Data availability**

529 The whole genome sequencing data were deposited at the European Nucleotide Archive (ENA)
530 under accession id ERP115099 and TN-seq data in the short read archive (SRA) at the National
531 Center for Biotechnology Information (NCBI) under BioProject ID PRJNA544248. Analyzed tables can
532 be found in the supplementary files. For other data, please contact the corresponding author.

533 **Material and Methods**

534 **Growth of bacteria**

535 *E. coli* and *S. aureus* strains were streaked from frozen stock onto Lysogenic Broth (LB) or Tryptic
536 Soya agar (TSA) plates, respectively. For all *E. coli* and most *S. aureus* experiments, the bacteria were
537 grown in LB medium (LB normal, LBN, 10 g Tryptone, 5 g Yeast extract, 5 g NaCl) pH 7.5 or LB medium
538 with extra 0.25 M, 0.5 M NaCl, 0.5 M KCl or 1 M sucrose added. For molecular cloning and some
539 other experiments (as indicated in the text), *S. aureus* strains were grown in TSB medium. Growth

540 curves were done in 125 ml flasks with 20 ml of medium without antibiotics. Cultures were
541 inoculated from overnight cultures to a starting OD_{600} of 0.01 and growth was followed by
542 determining OD_{600} readings every one or two hours.

543 **TN-seq experiments**

544 A previously published highly-saturated *S. aureus* USA300 library with a mix of six different
545 transposons was used [34, 35]. In addition, a new transposon library with only the blunt transposon,
546 containing approximately 1.2 million individual clones, was produced using the same techniques as
547 described in Santiago *et al.* [34].
548 In the first experiment (replicate A), a tube of the mixed library was thawed on ice and used to set
549 up a 20 ml pre-culture in LBN/Erm 5 µg/ml with a starting OD_{600} of 0.1. This starter culture was
550 grown for 1 hour and subsequently used to inoculate 25 ml of either LBN, LB 0.25 M NaCl or LB 0.5
551 M NaCl containing Erm 5 µg/ml to a starting OD_{600} of 0.00125. When the cultures reached an OD_{600}
552 of approximately 1.4, bacteria from 10-12 ml culture were harvested by centrifugation (10
553 generation sample). For, the 17 generation sample, the first cultures were back-diluted 1:100-fold
554 into 25 ml fresh medium when they reached an OD_{600} of 0.3 and bacteria from 10-12 ml harvested
555 by centrifugation when the back-diluted culture reached an OD_{600} of 1.3 to 1.6 (17 generations). The
556 bacterial pellets were washed once with their respective growth medium and stored at -20°C for
557 further processing. In the second experiment (replicate B), the transposon library containing only
558 the blunt transposon was used, Erm was omitted after the pre-culture step and samples were only
559 collected at around 16 generations. In the third experiment, the blunt library was used, Erm 10
560 µg/ml was only added to the pre-culture, and the bacteria grown in either LBN, LB 0.5 M NaCl, LB
561 0.5 M KCl or LB 1.0 M sucrose medium and cells collected after 16 generations.
562 The library preparation for sequencing was done as described previously [34]. Briefly, genomic DNA
563 was isolated, cut with *Not*I, biotinylated adapters ligated, the DNA cut again with *Mme*I, and

564 fragments ligated to Illumina adapters and the products PCR amplified, incorporating bar codes and
565 the Illumina adaptor sequences P5 and P7. The samples were sequenced on an Illumina HiSeq
566 machine after spiking with 40% PhiX DNA. The data analysis was done using the Tufts Galaxy Server
567 and custom python scripts as described earlier [34]. To this end, the reads were trimmed up to the
568 barcode and de-multiplexed by strain barcode. Due to the variability in the DNA cleavage by the
569 *Mme*I restriction enzyme, the reads that could not be mapped to a barcode were trimmed by an
570 additional base and the process repeated. Reads were then mapped to the USA300_TCH1516
571 (CP000730.1) genome and a hop table was generated. Statistical analysis (Mann-Whitney tests and
572 Benjamini-Hochberg) was done using custom python scripts [34]. Further exploration of the data
573 was done using Excel and custom R scripts.

574 ***S. aureus* cell diameter measurements**

575 For cell diameter measurements, *S. aureus* strains ANG4054, ANG4340, ANG4341 were grown
576 overnight (14-20 hours) at 37°C with 180 rpm shaking in 5 ml LBN in the presence of 100 ng/ml Atet.
577 100 µl of these overnight cultures was transferred to a 1.5 ml reaction tube and 1.5 µl of BODIPY-
578 FL-vancomycin (100 µg/ml in phosphate buffered saline) was added to each tube to stain the cell
579 wall. After a 30 min static incubation step at 37°C, 1.5 µl of the suspension was pipetted onto a slide
580 covered with a 1% agarose pad and analyzed by microscopy using an Axio Imager.A2 microscope
581 with an EC Plan-Neofluar 100x/1.30 Oil M27 objective and images recorded using an AxioCam MR
582 R3. Native CZI files were opened in FIJI [63] and cell diameters of 200 cells were measured using the
583 line and measure tool. Only cells without any visible septa were measured. Experiment was
584 conducted five times with independent biological cultures (n=5, 200 cells each).

585 **CFU/OD correlations**

586 The different *S. aureus* strains were grown as described for the cell diameter measurements. Optical
587 densities of cultures were measured as well as 100 µl of 10^{-6} dilutions (made in their respective
588 growth medium) plated onto TSA plates. The next day, the number of colonies were counted and
589 the ratios of OD_{600} to CFU calculated. The experiment was conducted six time with independent
590 biological samples (n=6).

591 **Zymogram assays**

592 The different *S. aureus* strains were grown over night in TSB. The next day, the bacteria from an
593 OD_{600} equivalent of 20 were pelleted by centrifugation for 3 min at 17000 x *g*. The cells were washed
594 twice with 600 µl PBS and subsequently suspended in 50 µl SDS sample buffer. The suspension was
595 boiled for 20 min with interspersed shaking, centrifuged for 5 min at 17000 x *g* and 20 µl of each
596 sample was loaded onto Zymogram gels, which where were prepared as described previously [64].
597 Gels were stained and de-stained using methylene blue and water. The experiment was performed
598 twice, and a representative result is shown.

599 **WTA isolation and analysis**

600 Overnight cultures of *S. aureus* strains ANG4054, ANG4340, ANG4341, ANG1575, ANG4290,
601 ANG4748, ANG4749, ANG4759 were prepared in LBN and used to inoculate 50 ml LBN or LB 0.4 M
602 NaCl to an OD_{600} of 0.01. The cultures were incubated at 37°C with shaking until they reached an
603 OD_{600} of 5 to 6. Where appropriate, 10 µg/ml chloramphenicol and 100 ng/ml Atet was also added
604 to the medium. The bacteria from 20-24 ml culture were harvested by centrifugation for 10 min at
605 7000 x *g*. The bacterial pellets were washed with 50 mM 2-(N-morpholino) ethanesulfonic acid
606 (MES) pH 6.5 buffer and stored at -20°C until further use. Pellets were then processed and WTA

607 separated on a 20% native polyacrylamide gel by electrophoresis on a Biorad Protein XL ii cell as
608 described previously [65] and WTA visualized by silver staining according to the manufacturer
609 protocol. Experiments were done with three biological replicates (n=3) and a representative result
610 is shown.

611 **Peptidoglycan isolation and analysis**

612 Peptidoglycan was prepared as described previously [66] with the following modifications: 0.5 L
613 (ANG4290, ANG4382, ANG4384) or 1.0 L (ANG5054, ANG4340, ANG4341) of LB 0.4 M NaCl medium
614 (all strains) or LBN (ANG5054, ANG4340, ANG4341) medium were inoculated to an OD_{600} of 0.01.
615 For strains carrying derivatives of plasmid piTET, the medium was supplemented with 100 ng/ml
616 Atet starting from the pre-cultures. The cultures were grown at 37°C with shaking at 180 rpm until
617 they reached an OD_{600} of 2-3 and bacteria were subsequently harvested by centrifugation.
618 Chromatography of mutanolysin digested peptidoglycan was performed as described previously
619 using an Agilent 1260 infinity system [66] and muropeptide peaks assigned according to de Jonge *et*
620 *al.* [67]. For the muropeptide quantification, a baseline was drawn, the total peak area determined
621 as well as the peak areas for mono- and the different multimer peaks and calculated as percentage
622 of the total peak area. The peak area quantification was done three times for each HPLC
623 chromatogram and average values were calculated. Experiments were done with three biological
624 replicates (n=3).

625 **Data analysis, software and statistics**

626 Data were processed with a combination of Python 3.6 (https://www.python.org), R 3.3 & 3.5
627 (https://www.r-project.org/), RStudio 1.1 & 1.2 (https://www.rstudio.com/), Prism 7 and 8
628 (https://www.graphpad.com), ChemStation OpenLab C.01.05 (https://www.agilent.com/) and
629 Microsoft Excel 15 and 16 (https://www.office.com/). Voronoi images were drawn using

630 Proteomaps V2 [36, 37] using custom TMD files. Microscopy images were analyzed using FIJI 1.0
631 (https://fiji.sc/). Statistical analysis was performed with Prism using appropriate tests as described
632 in the figure legends.

633 **Raising of Δ*957* suppressor strains**

634 Multiple independent overnight cultures of strain LAC*Δ*957* (ANG4290) were prepared in 5 ml LBN.
635 These cultures were back diluted the next day into 20 ml LB 0.5 M NaCl to a starting OD_{600} of 0.05
636 and grown for 8-10 hours at 37°C with shaking until the cultures were slightly turbid. 50 µl of each
637 culture was passed into 5 ml of LBN and grown overnight. The next day, appropriate culture dilutions
638 were plated onto LBN agar plates and incubated overnight at 37°C. For each independent culture,
639 multiple single colonies were picked and used to inoculate individual wells of a 96-well microtiter
640 plates containing 100 µl LBN and the plates were subsequently incubated at 37°C in a 96-well plate
641 incubator with shaking at 650 rpm. The next day, a culture aliquot was stored at -80°C, and the
642 cultures were also diluted 1:50 in LB 0.5 M NaCl medium and 20 µl of these diluted cultures used to
643 inoculate 180 µl of LB 0.5 M NaCl medium. The plates were incubated overnight with shaking at
644 37°C and the next morning the growth of the potential *957* suppressor strains compared to that of
645 the original LAC*Δ*957* deletion strain (ANG4290), which showed low growth and the WT LAC*
646 (ANG1575) strain, which showed good growth. For each lineage, four suppressors that showed good
647 growth were streaked out from the previously frozen stocks and subsequently single colonies
648 selected to set up overnight cultures. The deletion of gene *SAUSA300_0957* was confirmed by PCR
649 and after performing growth curves in culture flasks, one strain that showed significant growth
650 improvement compared to the original LAC*Δ*957* (ANG4290) strain was selected from each lineage.
651 These strains were streaked out again for single colonies and used to inoculate an overnight culture,
652 giving rise to the independently raised suppressor strains ANG4381 through ANG4394. The

653 compensatory mutations for several of these suppressor strains were subsequently determined by
654 whole genome sequencing.

655 **Transfer of *pbp2* SNPs by phage transduction**

656 In order to demonstrate that the SNPs in *pbp2* are responsible for the growth rescue of strain
657 LAC*Δ*957* (ANG4290), we transferred two different *pbp2* SNPs by phage transduction into the
658 original LAC*Δ*957* strain as well as repaired these SNPs in the suppressor strains. This was done by
659 placing an Erm-marked transposon in proximity of the *pbp*2 gene allowing at a certain frequency for
660 the co-transduction of the Erm marker and the *pbp2* SNP. To this end, the NTML transposon mutant
661 library strain NE789 [43] was used, which harbors a transposon insertion in *SAUSA300_1332*
662 (putative exonuclease) about 10 kbp upstream of the *pbp2* gene. *SAUSA300_1332* is expected to be
663 unrelated to salt stress and the cell wall synthesis machinery but close enough to lead to an
664 intermediate rate of co-transference with the *pbp2* SNPs. The transposon from NE789 was
665 transduced into WT LAC* [68] and strain LAC*Δ*957* (ANG4290) using phage Φ85 yielding strains
666 ANG4561 and ANG452, respectively. The transposon was also transduced into the suppressor
667 strains ANG4382 and ANG4384 transferring either *SAUSA300_1332::Tn* only, yielding strains
668 ANG4527 and 4528 or transferring *SAUSA300_1332::Tn* as well as replacing the *pbp2* SNP with a WT
669 *pbp2* allele yielding *pbp2* repaired strains ANG4557 and ANG4568. Lysates from strains ANG4527
670 and 4528 (suppressors containing *pbp2* SNPs and *SAUSA300_1332::Tn*) were used to transfer the
671 *pbp2* SNPs back into a clean LAC*Δ*957* strain background yielding strains ANG4624 and ANG4625
672 and into WT LAC*, yielding strains ANG4563 and ANG4564. Successful repair or transfer of the SNPs
673 was checked by PCR and subsequent restriction digest of the product choosing enzymes that
674 recognize sites present in either the WT or SNP allele (ANG4382 *pbp2* SNP: BsrI. Recognition site
675 CCWGG, additional site introduced by SNP; ANG4384 *pbp2* SNP: SspI. Recognition site: AATATT, site
676 missing in SNP).

677 **Determination of oxacillin MICs using Etest strips**

678 *S. aureus* strains LAC* piTET (ANG4054), LAC*Δ*957* piTET (ANG4340) and the complementation
679 strain LAC*Δ*957* piTET-*957* (ANG4341) were grown overnight (22 hours) in 5 ml TSB containing 10
680 µg/ml chloramphenicol and 100 ng/ml Atet. The next day, the cultures were diluted to an OD_{600} of
681 0.1 in sterile PBS buffer and streaked with cotton swabs onto cation adjusted Mueller-Hinton agar
682 plates supplemented with 2% NaCl and 100 ng/ml Atet. One M.I.C.Evaluator strip was placed on
683 each plate and the plates were incubated for 24 hours at 35°C. MICs were then read directly from
684 the strips. The experiment was done with 4 biological replicates (n=4).

685 **Moenomomycin growth improvement test**

686 *S. aureus* strains LAC* (ANG1575), LAC* Δ*957* (ANG4290), LAC* Δ*957* S2 (ANG4382) and LAC* Δ*957*
687 S4 (ANG4384) were grown overnight (18 hours) in 5 ml LBN. The next day, the cells were diluted to
688 an OD_{600} of 0.01 in LBN, grown until mid-exponential phase (OD_{600} 0.4-0.6) and normalized to an
689 OD_{600} of 0.1. The cells were 10-fold serially diluted and 5 µl of each dilution spotted onto LB agar
690 containing 0.5 M NaCl with either 0.02 µg/ml moenomycin (mix of moenomycin A, A12, C1, C3 and
691 C4, Santa Cruz Biotechnology) or no moenomycin. Plates were incubated at 37°C overnight (18-22
692 hours) and photographed. The experiment was done with 3 biological replicates (n=3) and one
693 representative result is shown.

694 **Whole genome sequencing**

695 Genomic DNA was either isolated using the Promega Gene Wizard kit according to the manufacturer
696 instructions or using chloroform-isoamylalcohol as described previously [69]. DNA was sent off for
697 whole genome sequencing to MicrobesNG, Birmingham, U.K. or libraries prepared using the
698 Illumina Nextera DNA kit and sequenced at the London Institute of Medical Sciences. Short reads

699 were trimmed in CLC workbench genomics (Qiagen), then mapped to a custom *S. aureus* USA300
700 LAC* reference genome generated in a previous study [70] and single nucleotide polymorphisms
701 called based on at least 80% frequency of occurrence. This list was compared to a manually curated
702 list of well non false-positives and these entries were removed.

703 **Nebraska Transposon Mutant Library (NTML) strains and complementation strains**

704 All Nebraska transposon mutant library (NTML) strains and primers used in this study are listed in
705 supplementary tables S8, S15 and S16. Transposon insertions in the respective genes were
706 confirmed by PCRs. For complementation analysis, NTML strains NE535 (JE2 *SAUSA300_0867*::*Tn*),
707 NE867 (JE2 *SAUSA300_0483*::*Tn*) were transformed as controls with the empty plasmid pCL55 [71],
708 yielding strains ANG4326 and ANG4328 and strains NE188 (JE2 *SAUSA300_0481*::*Tn*), NE251 (JE2
709 SAUSA300_0482::*Tn*), NE526 (JE2 *SAUSA300_0694*::*Tn*), NE736 (JE2 *SAUSA300_0910*::*Tn*), NE1384
710 (JE2 *SAUSA300_0957*::*Tn*) with plasmid piTET [72], yielding ANG4308, ANG4310, ANG4377,
711 ANG4336, ANG4338. The WT strain JE2 [43] was also transformed with both plasmids yielding JE2
712 pCL55 (ANG4325) and JE2 piTET (ANG4307).
713 The complementation plasmid piTET-*481* for strain NE188 (JE2 *SAUSA300_0481::Tn*) was
714 constructed by amplifying the *SAUSA300_0481* gene using primers P2378/P2379, digesting the
715 product with AvrII/BglII and ligating the fragment with plasmid piTET cut with the same enzymes.
716 The plasmid was then introduced into *E. coli* strain XL1-Blue, yielding ANG4139. After shuttling the
717 plasmid through *E. coli* strain IM08B [73], creating strain ANG4150, the plasmid was integrated into
718 the *geh* locus of NE188 (JE2 *SAUSA300_0481*::*Tn*) yielding strain ANG4309. The complementation
719 plasmid piTET-*482* for strain NE251 (JE2 SAUSA300_0482::*Tn*), piTET-*694* for strain NE526 (JE2
720 *SAUSA300_0694*::*Tn*), piTET-*910* for strain NE736 (JE2 *SAUSA300_0910*::*Tn*), and piTET-*957* for
721 strain NE1384 (JE2 *SAUSA300_0957*::*Tn*) were constructed in a similar manner using primer pairs
722 P2380/P2381 (*SAUSA300_0482*), P2388/P2389 (*SAUSA300_0694*), P2384/P2385 (*SAUSA300_0910*)

723 and P2386/P2387 (*SAUSA300_0957*), respectively. The complementation plasmids were recovered
724 in *E. coli* XL1-Blue yielding strains ANG4140 (SAUSA300_0482), ANG4142 (*SAUSA300_0694*),
725 ANG4144 (*SAUSA300_0910*) and ANG4145 (*SAUSA300_0957*), shuttled through *E. coli* IM08B giving
726 strains ANG4151 (*SAUSA300_0482*), ANG4153 (*SAUSA300_0694*), ANG4155 (*SAUSA300_0910*) and
727 ANG4156 (*SAUSA300_0957*) and finally introduced in the respective NTML strain yielding the
728 complementation strains ANG4311 (*SAUSA300_0482*), ANG4378 (*SAUSA300_0694*), ANG4337
729 (*SAUSA300_0910*) and ANG4339 (*SAUSA300_0957*).
730 Complementation plasmid pCL55-*483* for strain NE867 (JE2 *SAUSA300_0483*::*Tn*) was made by
731 fusing PCR products of the operon promoter (in front of *SAUSA300_0481*) amplified with primers
732 P2588/P2553 and the *SAUSA300_0483* gene, amplified with primers P2554/P2589 together using
733 primers P2588/P2589. The resulting fragment was cloned into pCL55 using EcoRI/BamHI restriction
734 sites. The plasmid was recovered in XL1-Blue, creating strain ANG4291, shuttled through *E. coli*
735 IM08B (ANG4292) and subsequently introduced into NE867 (JE2 *SAUSA300_0483*::*Tn*) to create
736 strain ANG4327. The complementation plasmid pCL55-*867* for strain NE535 (JE2
737 *SAUSA300_0867*::*Tn*) was constructed in a similar manner, using primers P2590/P2556 and
738 P2557/P2591 to amplify the promoter and *SAUSA300_0867* gene, which were subsequently fused
739 in a second PCR using primers P2590/P2591. The resulting fragment was cloning into pCL55 using
740 EcoRI/BamHI restriction sites and the resulting plasmid recovered in *E. coli* XL1-Blue (ANG4293),
741 shuttling through IM08B (ANG4294) and finally introduced into NE535 (JE2 *SAUSA300_0867*::*Tn*),
742 creating the complementation strain ANG4329.

743 **Construction of *S. aureus* gene deletion and complementation strains**

744 *S. aureus* strains with in-frame gene deletions were constructed by allelic exchange using plasmids
745 pIMAY [73] and pIMAY* [38]. The gene deletion plasmids were designed to contain approximately

746 1000 bp up- and downstream regions around the deletion site, amplified from LAC* genomic DNA
747 [68], and the first and last 30 bp of the open reading frame to be deleted.
748 For construction of plasmid pIMAY-Δ*957*, the up- and downstream regions of *SAUSA300_0957* were
749 amplified using primers P2370/P2371 and P2372/P2373, spliced together in a second PCR using
750 primers P2370/P2373 and cloned into pIMAY using XmaI/EcoRI. Plasmid pIMAY-Δ957 was recovered
751 in *E. coli* XL1-Blue, creating strain ANG4147, shuttled through *E. coli* IM08B (ANG4159) and
752 subsequently introduced into S*. aureus* LAC*Δ*957*. The allelic exchange to delete *SAUSA300_0957*
753 and to create strain LAC*Δ*957* (ANG4290) was performed as previously described [73]. For
754 complementation analysis, the above described plasmid piTET-*957* was integrated into the
755 chromosome of strain LAC*Δ*957*, giving rise to the complementation strain LAC*Δ*957* piTET-*957*
756 (ANG4341). As control, the empty plasmid piTET from ANG4163 was also integrated into the
757 chromosome of LAC*Δ*957* yielding strain LAC*Δ*957* piTET (ANG4340). The *lcpB* (SAUSA300_0958)
758 gene was deleted in a similar manner using primers P2844/P2845 and P2846/P2847 for the first and
759 primers P2844/P2847 for the second PCR and cloning the fragment XmaI/EcoRI into pIMAY. Plasmid
760 pIMAY-Δ*lcpB* was recovered in *E. coli* XL1blue (ANG4740), shuttled through *E. coli* IM08B (ANG4742)
761 and introduced into the *S. aureus* LAC* (ANG4744) and finally yielding the *lcpB* deletion strain
762 LAC*Δ*lcpB* (ANG4748).
763 Plasmid pIMAY*-Δ*957-958* was constructed for the production of an *SAUSA300_0957-0958* (*lcpB*)
764 double mutant strain in which the first 30 bases of *SAUSA300_0957* are fused to the last 30 bp of
765 *SAUSA300_0958* (*lcpB*). This was done using primers P2844/P2848 and P2849/P2373 in the first and
766 primers P2844/P2373 in a second PCR. The fragment was cloned using XmaI/EcoRI into pIMAY* [38]
767 and the resulting plasmid pIMAY*-Δ*957-958* recovered in *E. coli* XL1-Blue (ANG4741). The plasmid
768 was shuttled through *E. coli* IM08B (ANG4743), introduced into *S. aureus* LAC* (ANG4745) and
769 following the allelic exchange procedure yielding the *S. aureus* strain LAC*Δ*957-958* (*lcpB*)
770 (ANG4749).

771 The plasmid pIMAY-Δ*mgtE* was designed to contain up- and downstream regions of
772 *SAUSA300_0910* (*mgtE*) fused together by the first and last 30 bp of the gene in order to create a
773 LAC*Δ*mgtE* mutant. For this, primer pairs P2374/P2375 and P2376/P2377 were used to amplify up-
774 and downstream regions and subsequently spliced together by PCR using primers P2374/P2377.
775 The PCR fragment was digested with XmaI/EcoRI and ligated into pIMAY cut with the same enzymes.
776 The plasmid pIMAY-Δ*mgtE* was recovered in *E. coli* XL1-Blue yielding strain ANG4146 and shuttled
777 through *E. coli* IM08B yielding strain ANG4158. The plasmid pIMAY-Δ*mgtE* was then introduced into
778 LAC* yielding strain LAC*Δ*SAUSA300_0910* (*mgtE*) (ANG4422) after the knockout procedure. To
779 create an empty vector-containing control strain and a plasmid-based complementation strain, the
780 plasmid piTET and piTET-*910* from strains ANG4163 and ANG4155 were isolated and used to
781 transform strain LAC*Δ*SAUSA300_0910* (*mgtE*) (ANG4422), yielding strains ANG4445 (LAC*Δ*mgtE*
782 piTET) and ANG4446 (LAC*Δ*mgtE* piTET-*mgtE)*.
783 The *tagO* gene (*SAUSA300_0731*) was inactivated using the targetron intron homing system [74] or
784 by allelic exchange using pIMAY* [38]. For the targetron mutagenesis, plasmid pNL9164-*tagO* was
785 produced by amplifying the upstream targetron fragment with primers P2887 and the EBS universal
786 primer (P2890) and the downstream fragment using primers P2888/P2889, the fragments were
787 fused using the IBS primer (P2887) and the EBS1d primer (P2888). The final fragment was cloned
788 using HindIII/BsrGI into pNL9164 [74]. Plasmid pNL9164-*tagO* was recovered in *E. coli* XL1-Blue,
789 yielding strain ANG4703, introduced into *E. coli* IM08B to give rise to strain ANG4704 and finally
790 introduced into *S. aureus* LAC* [68] to create strain LAC* pNL9164-*tagO* (ANG4751). The final *tagO*
791 targetron mutant strain LAC**tagO*::targetron (ANG4753) was generated using the method
792 described by Yao *et al.* [74]. For the construction of *S. aureus* strain LAC*Δ*tagO* with an in-frame
793 deletion in *tagO,* the allelic exchange plasmid pIMAY*-Δ*tagO* was used. To this end, up- and
794 downstream *tagO* fragments were produced using primer pairs P2883/P2884 and P2885/P2886 and
795 introduced by Gibson cloning into XmaI/EcoRI pre-cut pIMAY*. Plasmid pIMAY*-Δ*tagO* was

796 recovered in *E. coli* XL1-Blue, generating strain ANG4755. After shuttling through *E. coli* strain IM08B
797 (ANG4756), the plasmid was introduced into *S. aureus* LAC* to create strain ANG4757. Finally, the
798 *tagO* locus was deleted by allelic exchange, generating strain LAC*Δ*tagO* (ANG4759). Because initial
799 generation of the mutant failed, cells were plated unselectively onto TSA plates and incubated at
800 room temperature (18-25°C) for about two weeks to enable colony differentiation between WT and
801 Δ*tagO* mutant strains. Upon prolonged incubation, *tagO* mutant strain colonies have an opaque
802 appearance.
803

804 **References**

805 1. Wertheim HF, Melles DC, Vos MC, van Leeuwen W, van Belkum A, Verbrugh HA, et al. The
806 role of nasal carriage in *Staphylococcus aureus* infections. Lancet Infect Dis. 2005;5(12):751-62. Epub
807 2005/11/29. doi: 10.1016/S1473-3099(05)70295-4. PubMed PMID: 16310147.
808 2. Tong SY, Davis JS, Eichenberger E, Holland TL, Fowler VG, Jr. *Staphylococcus aureus*
809 infections: epidemiology, pathophysiology, clinical manifestations, and management. Clin Microbiol
810 Rev. 2015;28(3):603-61. Epub 2015/05/29. doi: 10.1128/CMR.00134-14. PubMed PMID: 26016486;
811 PubMed Central PMCID: PMCPMC4451395.
812 3. Measures JC. Role of amino acids in osmoregulation of non-halophilic bacteria. Nature.
813 1975;257(5525):398-400. Epub 1975/10/02. PubMed PMID: 241020.
814 4. Adams MR, Moss MO. 7.14.2 The Organism and its Characteristics. Food Microbiology (3rd
815 Edition): Royal Society of Chemistry; 2008.
816 5. Csonka LN. Physiological and genetic responses of bacteria to osmotic stress. Microbiol Rev.
817 1989;53(1):121-47. Epub 1989/03/01. PubMed PMID: 2651863; PubMed Central PMCID:
818 PMCPMC372720.

819 6. Csonka LN, Hanson AD. Prokaryotic osmoregulation: genetics and physiology. Annu Rev
820 Microbiol. 1991;45:569-606. Epub 1991/01/01. doi: 10.1146/annurev.mi.45.100191.003033.
821 PubMed PMID: 1741624.
822 7. Sleator RD, Hill C. Bacterial osmoadaptation: the role of osmolytes in bacterial stress and
823 virulence. FEMS Microbiol Rev. 2002;26(1):49-71. Epub 2002/05/15. doi: 10.1111/j.1574-
824 6976.2002.tb00598.x. PubMed PMID: 12007642.
825 8. Graham JE, Wilkinson BJ. *Staphylococcus aureus* osmoregulation: roles for choline, glycine
826 betaine, proline, and taurine. J Bacteriol. 1992;174(8):2711-6. Epub 1992/04/01. PubMed PMID:
827 1556089; PubMed Central PMCID: PMCPMC205912.
828 9. Christian JH, Waltho JA. The Composition of *Staphylococcus aureus* in Relation to the Water
829 Activity of the Growth Medium. J Gen Microbiol. 1964;35:205-13. Epub 1964/05/01. doi:
830 10.1099/00221287-35-2-205. PubMed PMID: 14179669.
831 10. Miller KJ, Zelt SC, Bae J-H. Glycine betaine and proline are the principal compatible solutes
832 of *Staphylococcus aureus*. Current Microbiology. 1991;23(3):131-7. doi: 10.1007/bf02091971.
833 11. Townsend DE, Wilkinson BJ. Proline transport in *Staphylococcus aureus*: a high-affinity
834 system and a low-affinity system involved in osmoregulation. J Bacteriol. 1992;174(8):2702-10. Epub
835 1992/04/01. PubMed PMID: 1556088; PubMed Central PMCID: PMCPMC205911.
836 12. Anderson CB, Witter LD. Glutamine and proline accumulation by *Staphylococcus aureus* with
837 reduction in water activity. Appl Environ Microbiol. 1982;43(6):1501-3. Epub 1982/06/01. PubMed
838 PMID: 7103493; PubMed Central PMCID: PMCPMC244260.
839 13. Bae JH, Miller KJ. Identification of two proline transport systems in *Staphylococcus aureus*
840 and their possible roles in osmoregulation. Appl Environ Microbiol. 1992;58(2):471-5. Epub
841 1992/02/01. PubMed PMID: 1610171; PubMed Central PMCID: PMCPMC195271.

842 14. Pourkomailian B, Booth IR. Glycine betaine transport by *Staphylococcus aureus*: evidence for
843 feedback regulation of the activity of the two transport systems. Microbiology. 1992;140 (Pt
844 11):3131-8. Epub 1994/11/01. doi: 10.1099/13500872-140-11-3131. PubMed PMID: 7812452.
845 15. Price-Whelan A, Poon CK, Benson MA, Eidem TT, Roux CM, Boyd JM, et al. Transcriptional
846 profiling of *Staphylococcus aureus* during growth in 2 M NaCl leads to clarification of physiological
847 roles for Kdp and Ktr K+ uptake systems. MBio. 2013;4(4). Epub 2013/08/22. doi:
848 10.1128/mBio.00407-13. PubMed PMID: 23963175; PubMed Central PMCID: PMCPMC3747578.
849 16. Scybert S, Pechous R, Sitthisak S, Nadakavukaren MJ, Wilkinson BJ, Jayaswal RK. NaCl-
850 sensitive mutant of *Staphylococcus aureus* has a Tn917-lacZ insertion in its ars operon. FEMS
851 Microbiol Lett. 2003;222(2):171-6. Epub 2003/05/29. doi: 10.1016/S0378-1097(03)00312-4.
852 PubMed PMID: 12770703.
853 17. Schwan WR, Lehmann L, McCormick J. Transcriptional activation of the *Staphylococcus*
854 *aureus* putP gene by low-proline-high osmotic conditions and during infection of murine and human
855 tissues. Infect Immun. 2006;74(1):399-409. Epub 2005/12/22. doi: 10.1128/IAI.74.1.399-409.2006.
856 PubMed PMID: 16368996; PubMed Central PMCID: PMCPMC1346636.
857 18. Vijaranakul U, Xiong A, Lockwood K, Jayaswal RK. Cloning and nucleotide sequencing of a
858 *Staphylococcus aureus* gene encoding a branched-chain-amino-acid transporter. Appl Environ
859 Microbiol. 1998;64(2):763-7. Epub 1998/02/17. PubMed PMID: 9464420; PubMed Central PMCID:
860 PMCPMC106115.
861 19. Wengender PA, Miller KJ. Identification of a PutP proline permease gene homolog from
862 *Staphylococcus aureus* by expression cloning of the high-affinity proline transport system in
863 Escherichia coli. Appl Environ Microbiol. 1995;61(1):252-9. Epub 1995/01/01. PubMed PMID:
864 7887605; PubMed Central PMCID: PMCPMC167280.
865 20. Wetzel KJ, Bjorge D, Schwan WR. Mutational and transcriptional analyses of the
866 *Staphylococcus aureus* low-affinity proline transporter OpuD during *in vitro* growth and infection of

867 murine tissues. FEMS Immunol Med Microbiol. 2011;61(3):346-55. Epub 2011/01/15. doi:
868 10.1111/j.1574-695X.2011.00781.x. PubMed PMID: 21231964; PubMed Central PMCID:
869 PMCPMC3055929.
870 21. Zeden MS, Schuster CF, Bowman L, Zhong Q, Williams HD, Gründling A. Cyclic di-adenosine
871 monophosphate (c-di-AMP) is required for osmotic regulation in *Staphylococcus aureus* but
872 dispensable for viability in anaerobic conditions. J Biol Chem. 2018;293(9):3180-200. Epub
873 2018/01/13. doi: 10.1074/jbc.M117.818716. PubMed PMID: 29326168; PubMed Central PMCID:
874 PMCPMC5836111.
875 22. Vijaranakul U, Nadakavukaren MJ, de Jonge BL, Wilkinson BJ, Jayaswal RK. Increased cell size
876 and shortened peptidoglycan interpeptide bridge of NaCl-stressed *Staphylococcus aureus* and their
877 reversal by glycine betaine. J Bacteriol. 1995;177(17):5116-21. Epub 1995/09/01. PubMed PMID:
878 7665491; PubMed Central PMCID: PMCPMC177291.
879 23. Onyango LA, Hugh Dunstan R, Roberts TK, Macdonald MM, Gottfries J. Phenotypic variants
880 of staphylococci and their underlying population distributions following exposure to stress. PLoS
881 One. 2013;8(10):e77614. Epub 2013/11/10. doi: 10.1371/journal.pone.0077614. PubMed PMID:
882 24204894; PubMed Central PMCID: PMCPMC3799968.
883 24. Vollmer W, Blanot D, de Pedro MA. Peptidoglycan structure and architecture. FEMS
884 Microbiol Rev. 2008;32(2):149-67. Epub 2008/01/16. doi: 10.1111/j.1574-6976.2007.00094.x.
885 PubMed PMID: 18194336.
886 25. Madiraju MV, Brunner DP, Wilkinson BJ. Effects of temperature, NaCl, and methicillin on
887 penicillin-binding proteins, growth, peptidoglycan synthesis, and autolysis in methicillin-resistant
888 *Staphylococcus aureus*. Antimicrob Agents Chemother. 1987;31(11):1727-33. Epub 1987/11/01.
889 PubMed PMID: 3435121; PubMed Central PMCID: PMCPMC175029.
890 26. Stapleton MR, Horsburgh MJ, Hayhurst EJ, Wright L, Jonsson IM, Tarkowski A, et al.
891 Characterization of IsaA and SceD, two putative lytic transglycosylases of *Staphylococcus aureus*. J

892 Bacteriol. 2007;189(20):7316-25. Epub 2007/08/07. doi: 10.1128/JB.00734-07. PubMed PMID:
893 17675373; PubMed Central PMCID: PMCPMC2168438.
894 27. Ochiai T. Staphylococcus aureus produces autolysin-susceptible cell walls during growth in a
895 high-NaCl and low-Ca2+ concentration medium. Microbiol Immunol. 2000;44(2):97-104. Epub
896 2000/05/10. PubMed PMID: 10803496.
897 28. Koprivnjak T, Mlakar V, Swanson L, Fournier B, Peschel A, Weiss JP. Cation-induced
898 transcriptional regulation of the dlt operon of *Staphylococcus aureus*. J Bacteriol.
899 2006;188(10):3622-30. Epub 2006/05/05. doi: 10.1128/JB.188.10.3622-3630.2006. PubMed PMID:
900 16672616; PubMed Central PMCID: PMCPMC1482844.
901 29. Mistretta N, Brossaud M, Telles F, Sanchez V, Talaga P, Rokbi B. Glycosylation of
902 *Staphylococcus aureus* cell wall teichoic acid is influenced by environmental conditions. Sci Rep.
903 2019;9(1):3212. Epub 2019/03/03. doi: 10.1038/s41598-019-39929-1. PubMed PMID: 30824758;
904 PubMed Central PMCID: PMCPMC6397182.
905 30. Kho K, Meredith TC. Salt-Induced Stress Stimulates a Lipoteichoic Acid-Specific Three-
906 Component Glycosylation System in *Staphylococcus aureus*. J Bacteriol. 2018;200(12). Epub
907 2018/04/11. doi: 10.1128/JB.00017-18. PubMed PMID: 29632092; PubMed Central PMCID:
908 PMCPMC5971477.
909 31. Stewart CM, Cole MB, Legan JD, Slade L, Schaffner DW. Solute-specific effects of osmotic
910 stress on *Staphylococcus aureus*. J Appl Microbiol. 2005;98(1):193-202. Epub 2004/12/22. doi:
911 10.1111/j.1365-2672.2004.02445.x. PubMed PMID: 15610432.
912 32. Stewart CM, Cole MB, Legan JD, Slade L, Vandeven MH, Schaffner DW. *Staphylococcus*
913 *aureus* growth boundaries: moving towards mechanistic predictive models based on solute-specific
914 effects. Appl Environ Microbiol. 2002;68(4):1864-71. Epub 2002/03/28. doi:
915 10.1128/aem.68.4.1864-1871.2002. PubMed PMID: 11916706; PubMed Central PMCID:
916 PMCPMC123857.

917 33. Mitchell P, Moyle J. Permeability of the envelopes of *Staphylococcus aureus* to some salts,
918 amino acids, and non-electrolytes. J Gen Microbiol. 1959;20(2):434-41. Epub 1959/04/01. doi:
919 10.1099/00221287-20-2-434. PubMed PMID: 13654736.
920 34. Santiago M, Matano LM, Moussa SH, Gilmore MS, Walker S, Meredith TC. A new platform
921 for ultra-high density *Staphylococcus aureus* transposon libraries. BMC Genomics. 2015;16:252. doi:
922 10.1186/s12864-015-1361-3. PubMed PMID: 25888466; PubMed Central PMCID:
923 PMCPMC4389836.
924 35. Coe KA, Lee W, Komazin-Meredith G, Meredith TC, Grad YH, Walker S. Comparative Tn-Seq
925 reveals common daptomycin resistance determinants in *Staphylococcus aureus* despite strain-
926 dependent differences in essentiality of shared cell envelope genes. bioRxiv. 2019:648246. doi:
927 10.1101/648246.
928 36. Liebermeister W, Noor E, Flamholz A, Davidi D, Bernhardt J, Milo R. Visual account of protein
929 investment in cellular functions. Proc Natl Acad Sci U S A. 2014;111(23):8488-93. Epub 2014/06/04.
930 doi: 10.1073/pnas.1314810111. PubMed PMID: 24889604; PubMed Central PMCID:
931 PMCPMC4060655.
932 37. Otto A, Bernhardt J, Meyer H, Schaffer M, Herbst FA, Siebourg J, et al. Systems-wide
933 temporal proteomic profiling in glucose-starved Bacillus subtilis. Nat Commun. 2010;1:137. Epub
934 2011/01/27. doi: 10.1038/ncomms1137. PubMed PMID: 21266987; PubMed Central PMCID:
935 PMCPMC3105300.
936 38. Schuster CF, Howard SA, Gründling A. Use of the counter selectable marker PheS* for
937 genome engineering in *Staphylococcus aureus*. Microbiology. 2019. Epub 2019/04/04. doi:
938 10.1099/mic.0.000791. PubMed PMID: 30942689.
939 39. Ishibashi M, Kurokawa K, Nishida S, Ueno K, Matsuo M, Sekimizu K. Isolation of temperature-
940 sensitive mutations in *murC* of *Staphylococcus aureus*. FEMS Microbiology Letters. 2007;274(2):204-
941 9. doi: 10.1111/j.1574-6968.2007.00829.x.

942 40. Mlynek KD, Callahan MT, Shimkevitch AV, Farmer JT, Endres JL, Marchand M, et al. Effects
943 of Low-Dose Amoxicillin on Staphylococcus aureus USA300 Biofilms. Antimicrob Agents Chemother.
944 2016;60(5):2639-51. Epub 2016/02/10. doi: 10.1128/AAC.02070-15. PubMed PMID: 26856828;
945 PubMed Central PMCID: PMCPMC4862544.
946 41. Brown S, Santa Maria JP, Jr., Walker S. Wall teichoic acids of gram-positive bacteria. Annu
947 Rev Microbiol. 2013;67:313-36. doi: 10.1146/annurev-micro-092412-155620. PubMed PMID:
948 24024634; PubMed Central PMCID: PMCPMC3883102.
949 42. Vaish M, Price-Whelan A, Reyes-Robles T, Liu J, Jereen A, Christie S, et al. Roles of
950 *Staphylococcus aureus* Mnh1 and Mnh2 Antiporters in Salt Tolerance, Alkali Tolerance, and
951 Pathogenesis. J Bacteriol. 2018;200(5). Epub 2017/12/22. doi: 10.1128/JB.00611-17. PubMed PMID:
952 29263099; PubMed Central PMCID: PMCPMC5809693.
953 43. Fey PD, Endres JL, Yajjala VK, Widhelm TJ, Boissy RJ, Bose JL, et al. A genetic resource for
954 rapid and comprehensive phenotype screening of nonessential *Staphylococcus aureus* genes. MBio.
955 2013;4(1):e00537-12. doi: 10.1128/mBio.00537-12. PubMed PMID: 23404398; PubMed Central
956 PMCID: PMCPMC3573662.
957 44. Mäder U, Nicolas P, Depke M, Pané-Farré J, Debarbouille M, van der Kooi-Pol MM, et al.
958 *Staphylococcus aureus* Transcriptome Architecture: From Laboratory to Infection-Mimicking
959 Conditions. PLoS Genet. 2016;12(4):e1005962. Epub 2016/04/02. doi:
960 10.1371/journal.pgen.1005962. PubMed PMID: 27035918; PubMed Central PMCID:
961 PMCPMC4818034.
962 45. Chan YG, Frankel MB, Dengler V, Schneewind O, Missiakas D. *Staphylococcus aureus* mutants
963 lacking the LytR-CpsA-Psr family of enzymes release cell wall teichoic acids into the extracellular
964 medium. J Bacteriol. 2013;195(20):4650-9. doi: 10.1128/JB.00544-13. PubMed PMID: 23935043;
965 PubMed Central PMCID: PMCPMC3807444.

966 46. Over B, Heusser R, McCallum N, Schulthess B, Kupferschmied P, Gaiani JM, et al. LytR-CpsA-
967 Psr proteins in *Staphylococcus aureus* display partial functional redundancy and the deletion of all
968 three severely impairs septum placement and cell separation. FEMS Microbiol Lett.
969 2011;320(2):142-51. doi: 10.1111/j.1574-6968.2011.02303.x. PubMed PMID: 21554381.
970 47. Schaefer K, Matano LM, Qiao Y, Kahne D, Walker S. In vitro reconstitution demonstrates the
971 cell wall ligase activity of LCP proteins. Nat Chem Biol. 2017;13(4):396-401. Epub 2017/02/07. doi:
972 10.1038/nchembio.2302. PubMed PMID: 28166208; PubMed Central PMCID: PMCPMC5362317.
973 48. Rahman MM, Hunter HN, Prova S, Verma V, Qamar A, Golemi-Kotra D. The *Staphylococcus*
974 *aureus* Methicillin Resistance Factor FmtA Is a d-Amino Esterase That Acts on Teichoic Acids. MBio.
975 2016;7(1):e02070-15. Epub 2016/02/11. doi: 10.1128/mBio.02070-15. PubMed PMID: 26861022;
976 PubMed Central PMCID: PMCPMC4752606.
977 49. Berger-Bächi B, Barberis-Maino L, Strässle A, Kayser FH. FemA, a host-mediated factor
978 essential for methicillin resistance in *Staphylococcus aureus*: molecular cloning and characterization.
979 Mol Gen Genet. 1989;219(1-2):263-9. PubMed PMID: 2559314.
980 50. Oshida T, Sugai M, Komatsuzawa H, Hong YM, Suginaka H, Tomasz A. A *Staphylococcus*
981 *aureus* autolysin that has an N-acetylmuramoyl-L-alanine amidase domain and an endo-beta-N-
982 acetylglucosaminidase domain: cloning, sequence analysis, and characterization. Proc Natl Acad Sci
983 U S A. 1995;92(1):285-9. PubMed PMID: 7816834; PubMed Central PMCID: PMCPMC42863.
984 51. Holland LM, Conlon B, O'Gara JP. Mutation of *tagO* reveals an essential role for wall teichoic
985 acids in *Staphylococcus epidermidis* biofilm development. Microbiology. 2011;157(Pt 2):408-18.
986 Epub 2010/11/06. doi: 10.1099/mic.0.042234-0. PubMed PMID: 21051486.
987 52. Wyke AW. Isolation of five penicillin-binding proteins from *Staphylococcus aureus*. FEMS
988 Microbiology Letters. 1984;22(2):133-8. doi: doi:10.1111/j.1574-6968.1984.tb00711.x.
989 53. Murakami K, Fujimura T, Doi M. Nucleotide sequence of the structural gene for the penicillin-
990 binding protein 2 of *Staphylococcus aureus* and the presence of a homologous gene in other

991 staphylococci. FEMS Microbiol Lett. 1994;117(2):131-6. doi: 10.1111/j.1574-6968.1994.tb06754.x.
992 PubMed PMID: 8181715.
993 54. Lovering AL, De Castro L, Strynadka NC. Identification of dynamic structural motifs involved
994 in peptidoglycan glycosyltransfer. J Mol Biol. 2008;383(1):167-77. doi: 10.1016/j.jmb.2008.08.020.
995 PubMed PMID: 18760285.
996 55. Ostash B, Walker S. Moenomycin family antibiotics: chemical synthesis, biosynthesis, and
997 biological activity. Nat Prod Rep. 2010;27(11):1594-617. Epub 2010/08/24. doi: 10.1039/c001461n.
998 PubMed PMID: 20730219; PubMed Central PMCID: PMCPMC2987538.
999 56. Mayer S, Steffen W, Steuber J, Götz F. The *Staphylococcus aureus* NuoL-like protein MpsA
1000 contributes to the generation of membrane potential. J Bacteriol. 2015;197(5):794-806. Epub
1001 2014/12/03. doi: 10.1128/JB.02127-14. PubMed PMID: 25448817; PubMed Central PMCID:
1002 PMCPMC4325100.
1003 57. Tomita A, Zhang M, Jin F, Zhuang W, Takeda H, Maruyama T, et al. ATP-dependent
1004 modulation of MgtE in Mg(2+) homeostasis. Nat Commun. 2017;8(1):148. Epub 2017/07/28. doi:
1005 10.1038/s41467-017-00082-w. PubMed PMID: 28747715; PubMed Central PMCID:
1006 PMCPMC5529423.
1007 58. Schuster CF, Bellows LE, Tosi T, Campeotto I, Corrigan RM, Freemont P, et al. The second
1008 messenger c-di-AMP inhibits the osmolyte uptake system OpuC in *Staphylococcus aureus*. Sci Signal.
1009 2016;9(441):ra81. Epub 2016/08/18. doi: 10.1126/scisignal.aaf7279. PubMed PMID: 27531650;
1010 PubMed Central PMCID: PMCPMC5248971.
1011 59. Chan YG, Kim HK, Schneewind O, Missiakas D. The capsular polysaccharide of *Staphylococcus*
1012 *aureus* is attached to peptidoglycan by the LytR-CpsA-Psr (LCP) family of enzymes. J Biol Chem.
1013 2014;289(22):15680-90. Epub 2014/04/23. doi: 10.1074/jbc.M114.567669. PubMed PMID:
1014 24753256; PubMed Central PMCID: PMCPMC4140922.

1015 60. Pöhlmann-Dietze P, Ulrich M, Kiser KB, Döring G, Lee JC, Fournier JM, et al. Adherence of
1016 *Staphylococcus aureus* to endothelial cells: influence of capsular polysaccharide, global regulator
1017 agr, and bacterial growth phase. Infect Immun. 2000;68(9):4865-71. Epub 2000/08/19. PubMed
1018 PMID: 10948098; PubMed Central PMCID: PMCPMC101683.
1019 61. Pinho MG, Filipe SR, de Lencastre H, Tomasz A. Complementation of the essential
1020 peptidoglycan transpeptidase function of penicillin-binding protein 2 (PBP2) by the drug resistance
1021 protein PBP2A in *Staphylococcus aureus*. J Bacteriol. 2001;183(22):6525-31. Epub 2001/10/24. doi:
1022 10.1128/JB.183.22.6525-6531.2001. PubMed PMID: 11673420; PubMed Central PMCID:
1023 PMCPMC95481.
1024 62. Ochiai T. *Staphylococcus aureus* requires increased level of Ca(2+) or Mn(2+) to grow
1025 normally in a high-NaCl/low-Mg(2+) medium. Microbiol Immunol. 2001;45(11):769-76. Epub
1026 2002/01/17. PubMed PMID: 11791670.
1027 63. Schindelin J, Arganda-Carreras I, Frise E, Kaynig V, Longair M, Pietzsch T, et al. Fiji: an open-
1028 source platform for biological-image analysis. Nat Methods. 2012;9(7):676-82. doi:
1029 10.1038/nmeth.2019. PubMed PMID: 22743772; PubMed Central PMCID: PMCPMC3855844.
1030 64. Atilano ML, Pereira PM, Vaz F, Catalão MJ, Reed P, Grilo IR, et al. Bacterial autolysins trim
1031 cell surface peptidoglycan to prevent detection by the *Drosophila* innate immune system. Elife.
1032 2014;3:e02277. doi: 10.7554/eLife.02277. PubMed PMID: 24692449; PubMed Central PMCID:
1033 PMCPMC3971415.
1034 65. Covas G, Vaz F, Henriques G, Pinho MG, Filipe SR. Analysis of Cell Wall Teichoic Acids in
1035 *Staphylococcus aureus*. Methods Mol Biol. 2016;1440(1440):201-13. doi: 10.1007/978-1-4939-
1036 3676-2_15. PubMed PMID: 27311674.
1037 66. Corrigan RM, Abbott JC, Burhenne H, Kaever V, Gründling A. c-di-AMP is a new second
1038 messenger in *Staphylococcus aureus* with a role in controlling cell size and envelope stress. PLoS

1039 Pathog. 2011;7(9):e1002217. doi: 10.1371/journal.ppat.1002217. PubMed PMID: 21909268;
1040 PubMed Central PMCID: PMCPMC3164647.
1041 67. de Jonge BL, Chang YS, Gage D, Tomasz A. Peptidoglycan composition of a highly methicillin-
1042 resistant *Staphylococcus aureus* strain. The role of penicillin binding protein 2A. J Biol Chem.
1043 1992;267(16):11248-54. PubMed PMID: 1597460.
1044 68. Boles BR, Thoendel M, Roth AJ, Horswill AR. Identification of genes involved in
1045 polysaccharide-independent *Staphylococcus aureus* biofilm formation. PLoS One.
1046 2010;5(4):e10146. doi: 10.1371/journal.pone.0010146. PubMed PMID: 20418950; PubMed Central
1047 PMCID: PMCPMC2854687.
1048 69. Schuster CF, Bertram R. Fluorescence based primer extension technique to determine
1049 transcriptional starting points and cleavage sites of RNases *in vivo*. J Vis Exp. 2014;(92):e52134. doi:
1050 10.3791/52134. PubMed PMID: 25406941; PubMed Central PMCID: PMCPMC4353401.
1051 70. Bowman L, Zeden MS, Schuster CF, Kaever V, Grundling A. New Insights into the Cyclic Di-
1052 adenosine Monophosphate (c-di-AMP) Degradation Pathway and the Requirement of the Cyclic
1053 Dinucleotide for Acid Stress Resistance in *Staphylococcus aureus*. J Biol Chem. 2016;291(53):26970-
1054 86. Epub 2016/11/12. doi: 10.1074/jbc.M116.747709. PubMed PMID: 27834680; PubMed Central
1055 PMCID: PMCPMC5207132.
1056 71. Lee CY, Buranen SL, Ye ZH. Construction of single-copy integration vectors for *Staphylococcus*
1057 *aureus*. Gene. 1991;103(1):101-5. PubMed PMID: 1652539.
1058 72. Gründling A, Schneewind O. Genes required for glycolipid synthesis and lipoteichoic acid
1059 anchoring in *Staphylococcus aureus*. J Bacteriol. 2007;189(6):2521-30. doi: 10.1128/JB.01683-06.
1060 PubMed PMID: 17209021; PubMed Central PMCID: PMCPMC1899383.
1061 73. Monk IR, Shah IM, Xu M, Tan MW, Foster TJ. Transforming the untransformable: application
1062 of direct transformation to manipulate genetically *Staphylococcus aureus* and *Staphylococcus*

1063 *epidermidis*. MBio. 2012;3(2). doi: 10.1128/mBio.00277-11. PubMed PMID: 22434850; PubMed
1064 Central PMCID: PMCPMC3312211.
1065 74. Yao J, Zhong J, Fang Y, Geisinger E, Novick RP, Lambowitz AM. Use of targetrons to disrupt
1066 essential and nonessential genes in *Staphylococcus aureus* reveals temperature sensitivity of Ll.LtrB
1067 group II intron splicing. RNA. 2006;12(7):1271-81. doi: 10.1261/rna.68706. PubMed PMID:
1068 16741231; PubMed Central PMCID: PMCPMC1484445.
1069
1070

1071 **Figure legends**

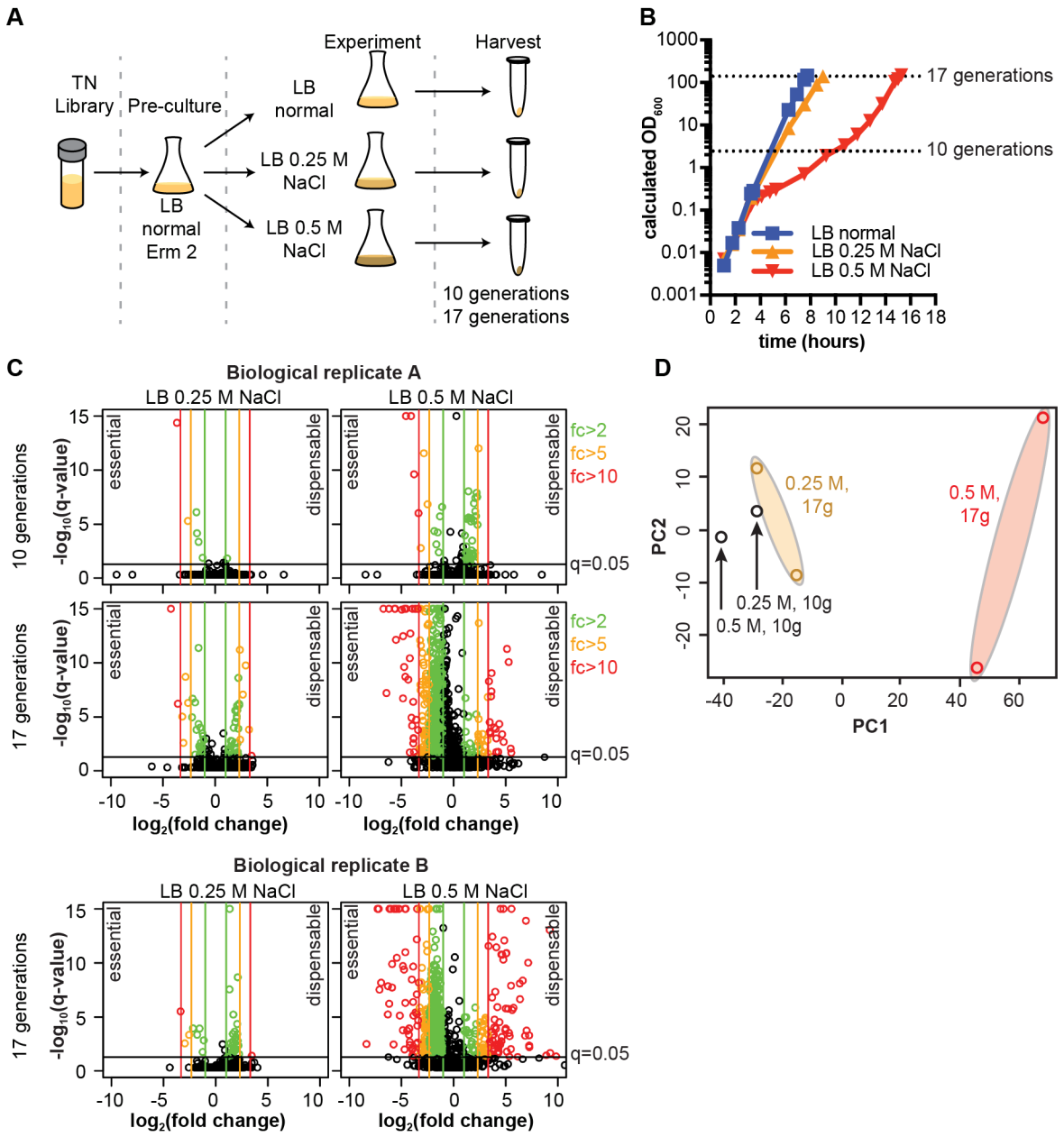

1072

1073 **Fig. 1. TN-Seq screen reveals essential and dispensable genes during prolonged NaCl stress in *S.***
1074 ***aureus*.**

1075 (A) Workflow of TN-seq experiments. A saturated transposon library was pre-cultured for one hour,

1076 then used to inoculate LB medium containing either normal levels (0.086 M), 0.25 M or 0.5 M of

1077 NaCl. After 10 and 17 generations, cells were harvested, and transposon insertion sites determined

1078 by high throughput sequencing.

1079 (B) Growth curve. Growth of the *S. aureus* library culture in LBN, LB 0.25 M NaCl and LB 0.5 M

1080 medium was followed by determining OD_{600} readings. Dotted lines indicate 10 and 17 generation

1081 thresholds. Cultures were back-diluted once when they reached an OD of approximately 0.3 and the
1082 optical densities shown are calculated from measured ODs time dilution factor. Culture from
1083 replicate B (n=1) is shown and a similar growth profile was seen for replicate A.
1084 (C) Volcano plots of essential and dispensable genes in NaCl conditions compared to LBN. Negative
1085 $\log_2$ fold-changes indicate essential and positive $\log_2$ fold-changes dispensable genes. q-value stands
1086 for Benjamini-Hochberg false discovery rate. Black horizontal line indicates q-value of 0.05 (cut-off)
1087 and red, orange and green vertical lines 10-, 5- and 2-fold differences in either direction. Colored
1088 circles indicate genes for which a significant change in the number of transposon insertions was
1089 observed above q-value cutoff and follow the same color code as the vertical lines. Bacteria in
1090 replicate A (top) were grown in 0.25 M and 0.5 M NaCl for 10 and 17 generations, whereas bacteria
1091 in replicate B (bottom) were only grown for 17 generations (n=1 for each plot).
1092 (D) Principal component analysis (PCA). A PCA was performed on the TN-seq data for replicates A
1093 and B shown in panel (C). The data for the 17 generation 0.25 M (orange) and 0.5 M NaCl (red)
1094 growth conditions clustered together, indicating good reproducibility between the two replicates.
1095

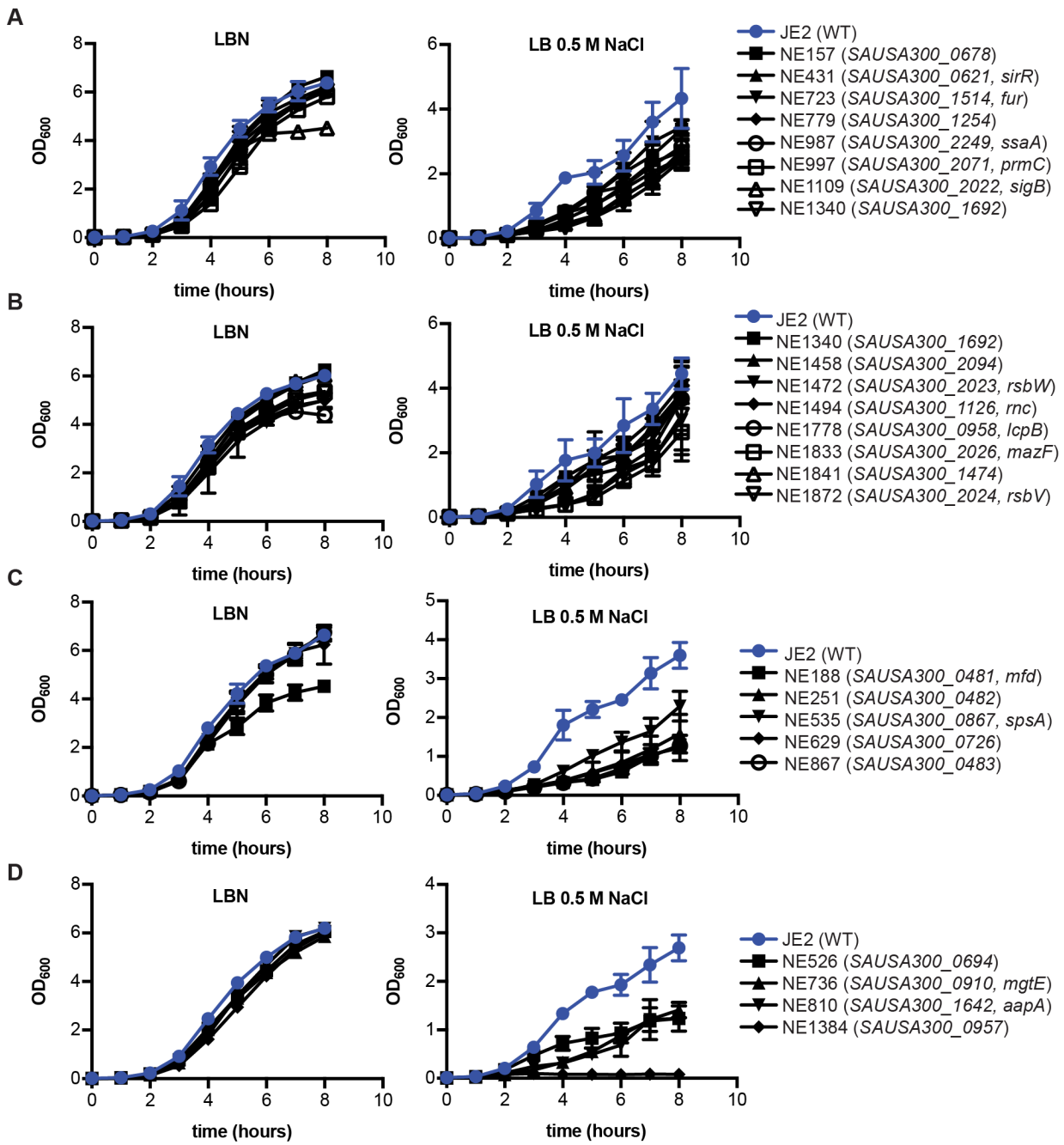

Fig. 2. Growth curves of *S. aureus* strains with transposon insertions in potential salt essential genes.

S. aureus strain JE2 (WT) and strains from the Nebraska Transposon Mutant Library (NTML) containing transposon insertions in potential salt essential genes were grown in LBN (left column) or 0.5 M NaCl LB medium (right column) and their growth monitored over 8 hours. Transposon mutant strains shown in panels (A) and (B) had a mild growth defect while strains shown in panels (C) and (D) had a stronger growth defect when grown in the high salt medium. NE numbers

1104 correspond to the NTML mutant number. Locus tag number and where available gene names with

1105 transposon insertion site are given in parenthesis. Growth curves were performed in triplicates

1106 (n=3) and means and SDs were plotted.

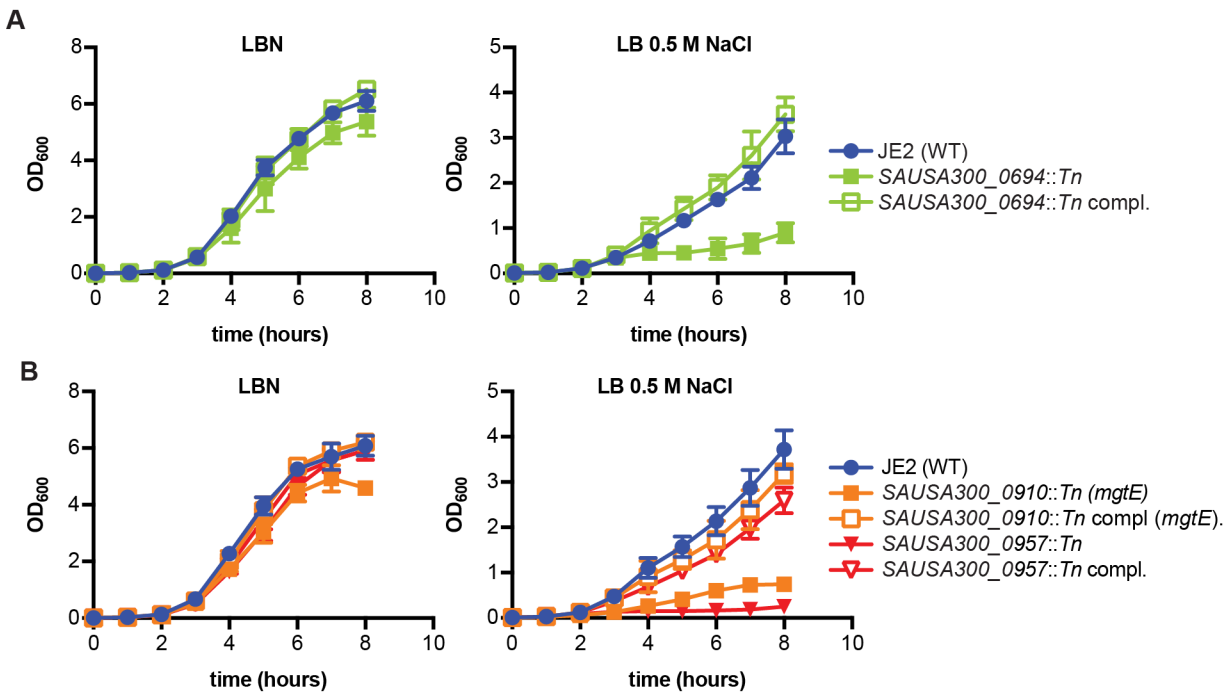

1107

1108 **Fig. 3. Growth curves and complementation analysis of *S. aureus* strains with transposon**

1109 **insertions in salt essential genes.**

1110 *S. aureus* strains (A) JE2 (WT), *SAUSA300_0694::Tn* mutant with empty plasmid and

1111 complementation strain or (B) JE2 (WT), *SAUSA300_0910* (*mgtE*), *SAUSA300_0957::Tn* with empty

1112 plasmid and respective complementation strains were grown in LBN (left panels) or LB 0.5 M NaCl

1113 medium (right panels) supplemented with 100 ng/ml Atet and OD_{600} readings determined at timed

1114 intervals. Growth curves were performed in triplicates (n=3) and means and SDs of OD_{600} readings

1115 were plotted.

1116

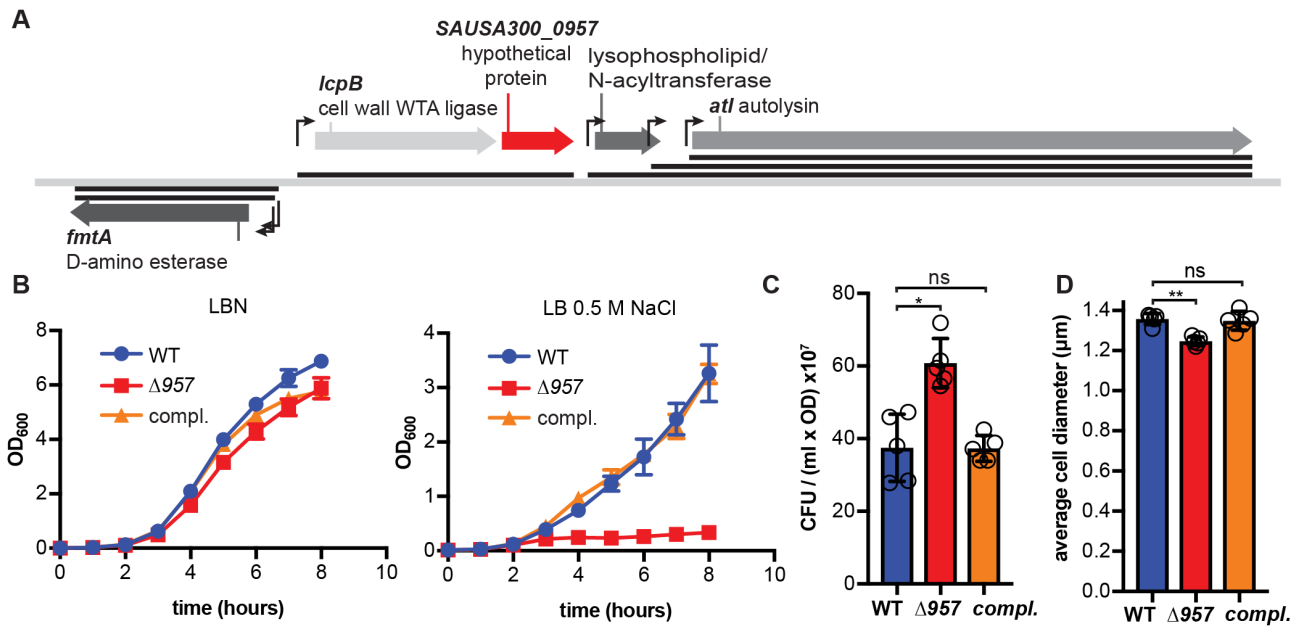

Fig. 4. Gene *SAUSA300_0957* is located in a genomic region with cell envelope genes and its deletion leads to salt sensitivity and other phenotypic changes.

(A) Schematic of the *S. aureus* USA300 FPR3757 chromosomal region with gene *SAUSA300_0957* (gene *957*). Gene *957* is encoded in an operon with *lcpB*, which codes for a wall teichoic acid ligase. *fmtA,* a proposed D-amino esterase acting on teichoic acid and genes coding for a predicted acyltransferase and the major autolysin Atl are located up and downstream of this operon. Putative promoters are shown as angled arrows (adapted from [44]) and black bars indicate the corresponding transcripts.

(B) Growth curves. *S. aureus* strains LAC* piTET (WT), LAC*Δ*957* piTET (Δ*957*) and the complementation strain LAC*Δ*957* piTET-*957* (compl.) were grown in LBN or LB containing 0.5 M NaCl medium and 100 ng/ml Atet. The growth was monitored by determining OD_{600} readings the means and SDs from three independent experiments were plotted.

(C) Determination of CFU/OD ratios. OD_{600} values as well as CFU/ml were determined for overnight cultures of the *S. aureus* strains described in panel (B) and the means and SDs of the CFU per ml OD_{600} of 1 from five independent experiments were plotted.

1134 (D) Cell size measurements. The cell walls of the *S. aureus* strains described in panel (B) were stained
1135 with fluorescently labelled vancomycin and the cells subsequently observed under a microscope.
1136 The diameters of 200 cells were measured and the means calculated. This average of the means and
1137 SDs from five independent experiments were plotted.
1138 For statistical analysis, a Kruskal-Wallis one-way ANOVA test was performed followed by a Dunn's
1139 post-hoc test to determine p-values. Asterisks (*) indicate $p \leq 0.05$ and two asterisks (**) $p \leq 0.01$ and
1140 ns=not significant.
1141

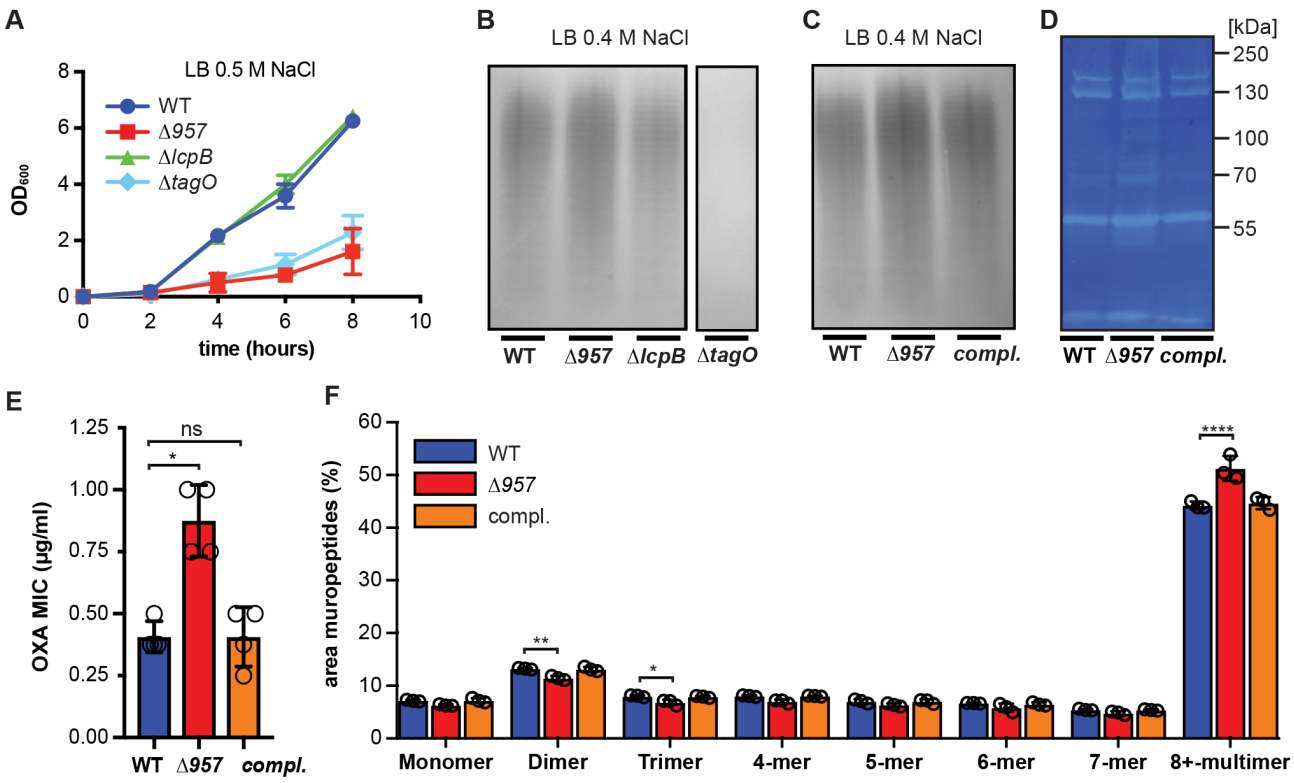

Fig. 5. Inactivation of gene 957 leads to an increase in peptidoglycan crosslinking.

(A) Growth curves. *S. aureus* strains LAC* (WT), LAC*Δ*957* (Δ*957*), LAC*Δ*lcpB*, (Δ*957*), and LAC*Δ*tagO* (Δ*tagO*) were grown in LB 0.5 M NaCl medium and OD_{600} readings determined at timed intervals. The means and SDs from three biological replicates were plotted.

(B) Detection of WTA on silver stained gels. WTA was isolated from *S. aureus* strains described in panel (A) following growth in LB 0.4 M NaCl medium. The WTA was separated by electrophoresis and visualized by silver stain. The experiment was performed three times and one representative gel image is shown.

(C) Detection of WTA on silver stained gels. Same as (B) but using the strains LAC* piTET (WT), LAC*Δ*957* piTET (Δ*957*), and the complementation strain LAC*Δ*957* piTET-*957* (compl.) grown in LB 0.4 M NaCl medium also containing 100 ng/ml Atet.

(D) Zymogram gel. Cell extracts prepared from *S. aureus* strains described in panel (C) were separated on a gel containing heat killed *Micrococcus luteus* cells. Autolysins were renatured and

1156 the zones of lysis visualized by methylene blue staining. The experiment was performed twice and
1157 one experiment is shown.
1158 (E) Determination of oxacillin MICs. Oxacillin MICs were determined for *S. aureus* strains described
1159 in panel (C) using Etest strips. The median and SDs from four biological replicates were plotted.
1160 (F) Muropeptide analysis. The same *S. aureus* strains as described in (C) were grown in LB 0.4 M
1161 NaCl medium also containing 100 ng/ml Atet, peptidoglycan isolated and digested with mutanolysin
1162 and the resulting muropeptide fragments separated by HPLC. Representative chromatograms are
1163 shown in Supplementary Figures S5E. The peak area of individual peaks (corresponding to monomer
1164 up to 8-mers and above) were quantified and the means and SDs from three biological replicates
1165 plotted.
1166 For statistical analysis of the oxacillin MICs in (E) a Kruskal-Wallis one-way ANOVA and a Dunn's
1167 post-hoc test was performed and for the muropeptide analysis in (F) a two-way ANOVA and a
1168 Dunnett's post-hoc test. One asterisk (*) indicates $p \leq 0.05$, two asterisks (**) $p \leq 0.01$ and four
1169 asterisks (****) $p \leq 0.0001$. ns=not significant.
1170

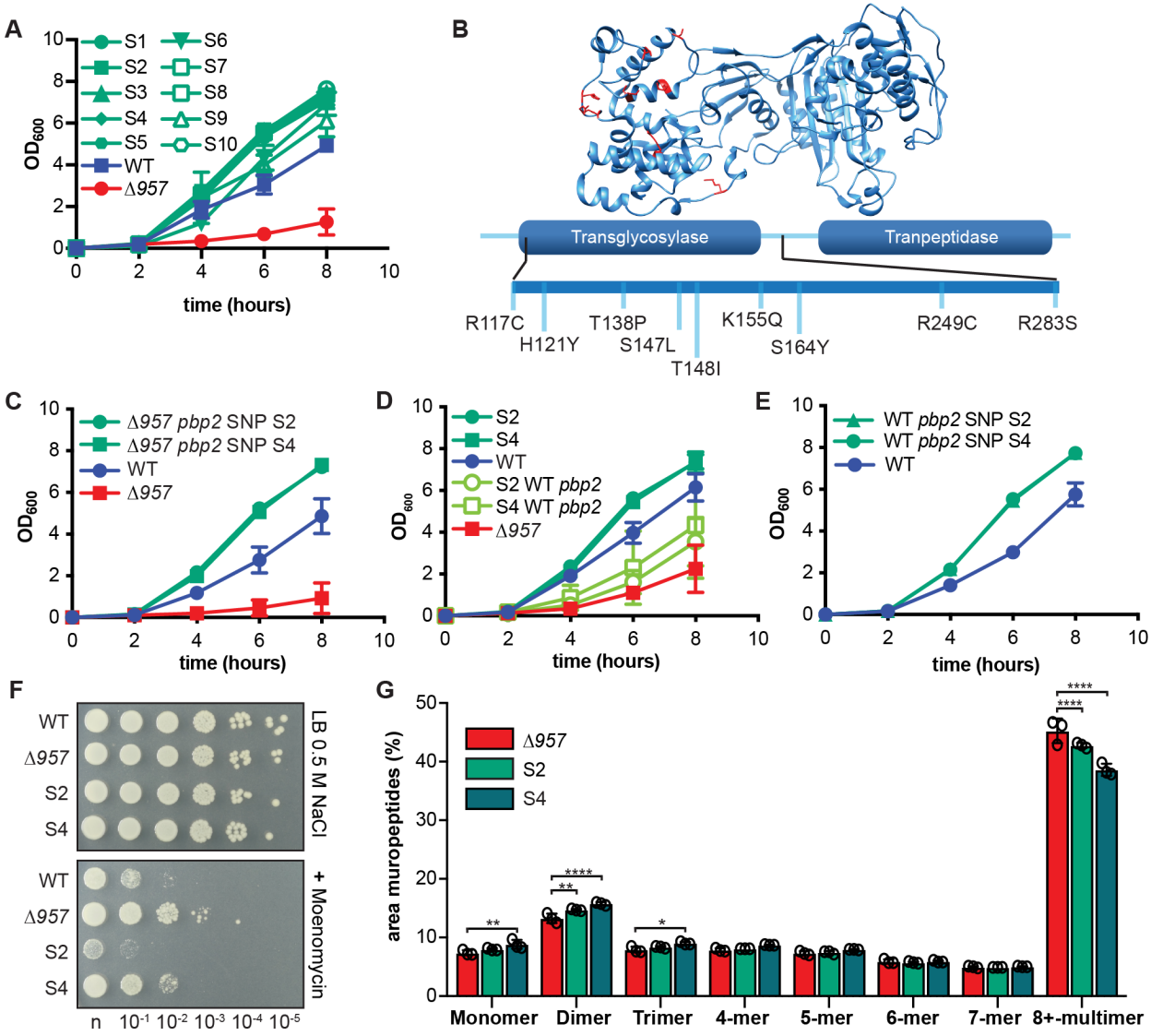

Fig. 6. The growth and peptidoglycan defect observed for the *957* mutant can be rescued by compensatory mutations in *pbp2*.

(A) Growth curves. *S. aureus* strains LAC* (WT), LAC*Δ*957* (Δ*957*) and the LAC*Δ*957* suppressors S1-10 (S1 to 10) were grown in LB 0.5 M NaCl medium, OD_{600} readings determined and the means and SDs of four biological replicates plotted.

(B) Schematic of Pbp2 with amino acid substitutions identified. Top: Structure of the *S. aureus* penicillin binding protein Pbp2 (PDB: 3DWK, [54]) with amino acids that are altered in the obtained suppressor strains shown in red. Bottom: Schematic of the Pbp2 enzyme with the transglycosylase

1180 and transpeptidase domains as well as the observed amino acid changes in the transglycosylase
1181 domain indicated.
1182 (C) Growth curves using *957* mutant strains containing *pbp2* alleles from suppressors S2 and S4.
1183 Growth curves were performed in LB 0.5 M NaCl medium and plotted as described in panel (A) but
1184 using *S. aureus* strains LAC* *1332*::Tn (WT), LAC*Δ*957* *1332*::Tn (Δ*957*), LAC*Δ*957* *1332*::Tn *pbp2*
1185 SNP S2 (Δ*957* *pbp2* SNP S2), LAC*Δ*957* suppressor S4 *1332*::Tn (Δ*957* *pbp2* SNP S4).
1186 (D) Growth curves using *957* suppressors with their *pbp2* gene repaired to WT. Growth curves were
1187 performed in LB 0.5 M NaCl medium and plotted as described in panel (A) but using *S. aureus* strains
1188 LAC* *1332*::Tn (WT), LAC*Δ*957* *1332*::Tn (Δ*957*), LAC*Δ*957* suppressor S2 *1332*::Tn (S2), LAC*Δ*957*
1189 suppressor S4 *1332*::Tn (S4), LAC*Δ*957* suppressor S2 *1332*::Tn repaired WT *pbp2* (S2 WT *pbp2*),
1190 and LAC*Δ*957* suppressor S4 *1332*::Tn repaired WT *pbp2* (S4 WT *pbp2*).
1191 (E) Growth curves using WT strains carrying *pbp2* SNPs. *S. aureus* strains LAC* *1332*::Tn (WT), LAC*
1192 *1332*::Tn *pbp2* SNP S2 (WT *pbp2* SNP S2) and LAC* *1332*::Tn *pbp2* SNP S4 (WT *pbp2* SNP S4) were
1193 grown in LB 0.5 M NaCl medium and OD_{600} readings determined and the means and SDs of three
1194 biological replicates plotted.
1195 (F) Bacterial growth on moenomycin supplemented agar plates. *S. aureus* strains LAC* (WT),
1196 LAC*Δ*957* (Δ*957*), LAC*Δ*957* Suppressor S2 (S2) and S4 LAC*Δ*957* Suppressor S4 (S4) were grown
1197 to exponential phase, normalized to an OD_{600} of 0.1 and plated either neat (n) or in 10-fold dilutions
1198 onto LB agar containing 0.5 M NaCl without (top) or with (bottom) moenomycin. Shown is one
1199 representative image of three biological replicates.
1200 (G) Muropeptide analysis. *S. aureus* strains LAC*Δ*957* (Δ*957*), LAC*Δ*957* Suppressor S2 (S2) and S4
1201 LAC*Δ*957* Suppressor S4 (S4) were grown in 0.4 M NaCl LB medium and muropeptides quantified
1202 as described in Fig 5F. Representative chromatograms are shown in Supplementary Figure S7D. The
1203 means and SDs from three biological replicates were plotted. For statistical analysis a two-way

1204 ANOVA and Dunnett's post-hoc test was performed. One asterisk (*) indicates $p \leq 0.05$, two asterisks

1205 (**) $p \leq 0.01$ and four asterisks (****) $p \leq 0.0001$.

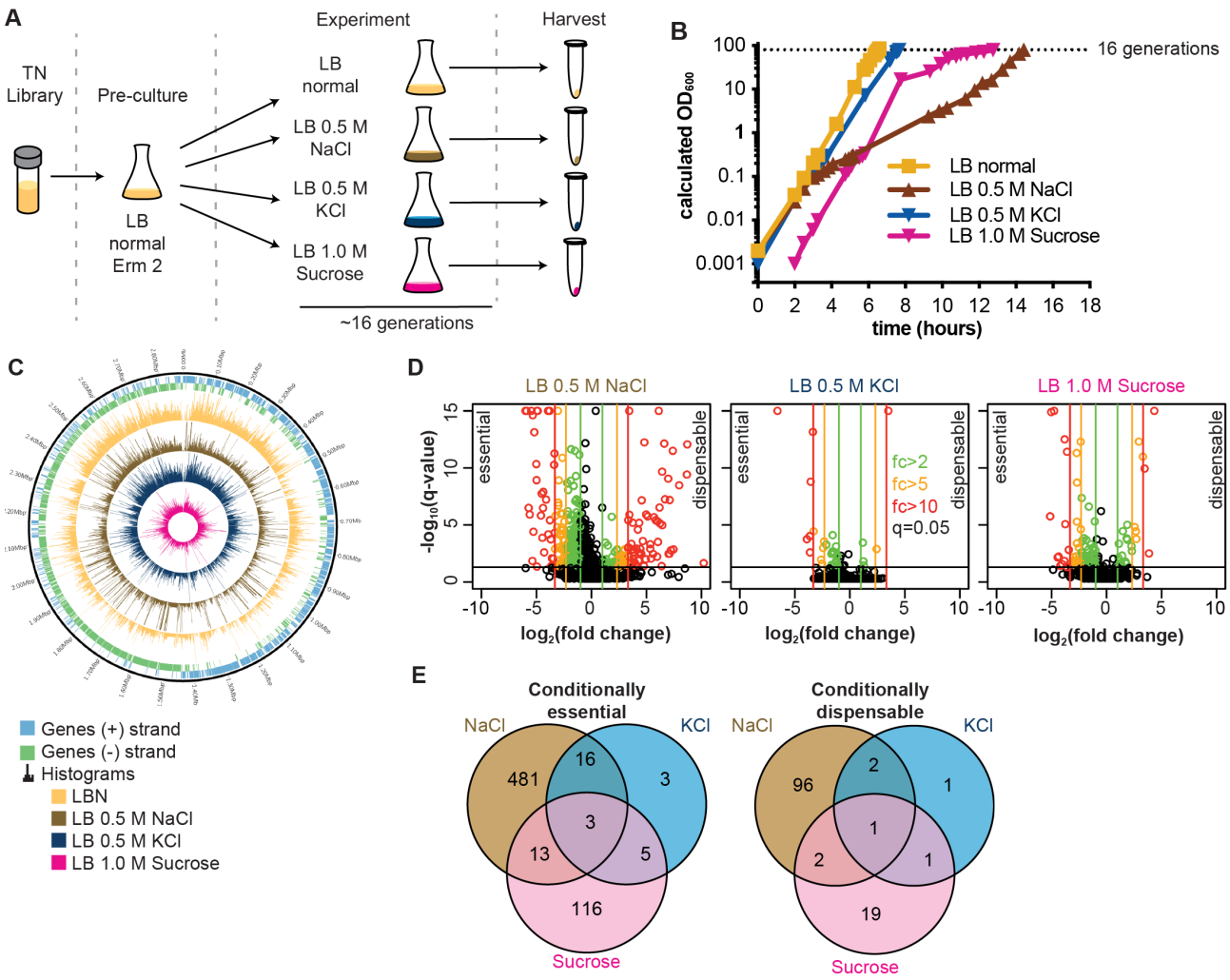

Fig. 7. Different sets of genes are conditionally essential for the growth of *S. aureus* under NaCl, KCl or sucrose stress conditions.

(A) Workflow of the TN-seq experiment. A TN-seq library was pre-cultured and then used to inoculate LBN, LB containing 0.5 M NaCl, 0.5 M KCl or 1 M sucrose. Cells were kept in exponential phase for 16 generations, harvested and transposon insertion sites determined by high throughput sequencing.

(B) Growth curves. For the TN-seq experiment (n=1), the growth of an *S. aureus* library cultured in LBN, LB 0.5M NaCl, LB 0.5 M KCl or LB 1.0 M sucrose medium was followed by taking OD_{600} measurements at timed intervals. The cultures were back-diluted once when they reached an OD_{600} of approximately 0.3. The plotted OD_{600} values were calculated by multiplying the measured OD_{600}

1217 with the dilution factor. The dotted line indicates the 16 generation cut-off at which cultures were
1218 harvested.
1219 (C) Circular plot showing the transposon insertion density along the *S. aureus* genome under
1220 different osmotic stress conditions. The two outer rings depict genes located on the (+) or (-) strand
1221 in *S. aureus* strain USA300 FPR3757. The inner four rings show the histograms of transposon
1222 insertions on a per gene basis after growth of the library in LBN (orange), 0.5 M NaCl (brown), 0.5
1223 M KCl (blue) and 1 M sucrose (pink) medium for 16 generations.
1224 (D) Volcano plots of conditionally essential and dispensable genes following growth of *S. aureus* in
1225 0.5 M NaCl, 0.5 M KCl or 1 M sucrose medium and compared to LBN conditions. q-values represent
1226 Benjamini-Hochberg corrected p-values, and $\log_2$ (fold changes) indicate essential genes (negative
1227 values) or dispensable genes (positive values). The black horizontal line indicates a q-value of 0.05,
1228 which was deemed the significance level. Vertical lines indicate 2- (green), 5- (orange) or 10- (red)
1229 fold changes in either direction. Each dot represents one gene and coloring follows the fold-change
1230 scheme whenever the q-value threshold was met. The TN-seq experiments were conducted once
1231 (n=1).
1232 (E) Venn diagrams showing overlaps of conditionally essential and dispensable genes during
1233 prolonged NaCl, KCl or sucrose stress. Genes with a 2-fold decrease (essential genes) or a 2-fold
1234 increase (dispensable genes) in transposon insertions under each stress condition compared to the
1235 LBN condition and a q-value of ≤0.05 were determined and the overlap between these gene lists
1236 displayed in Venn diagrams.
1237

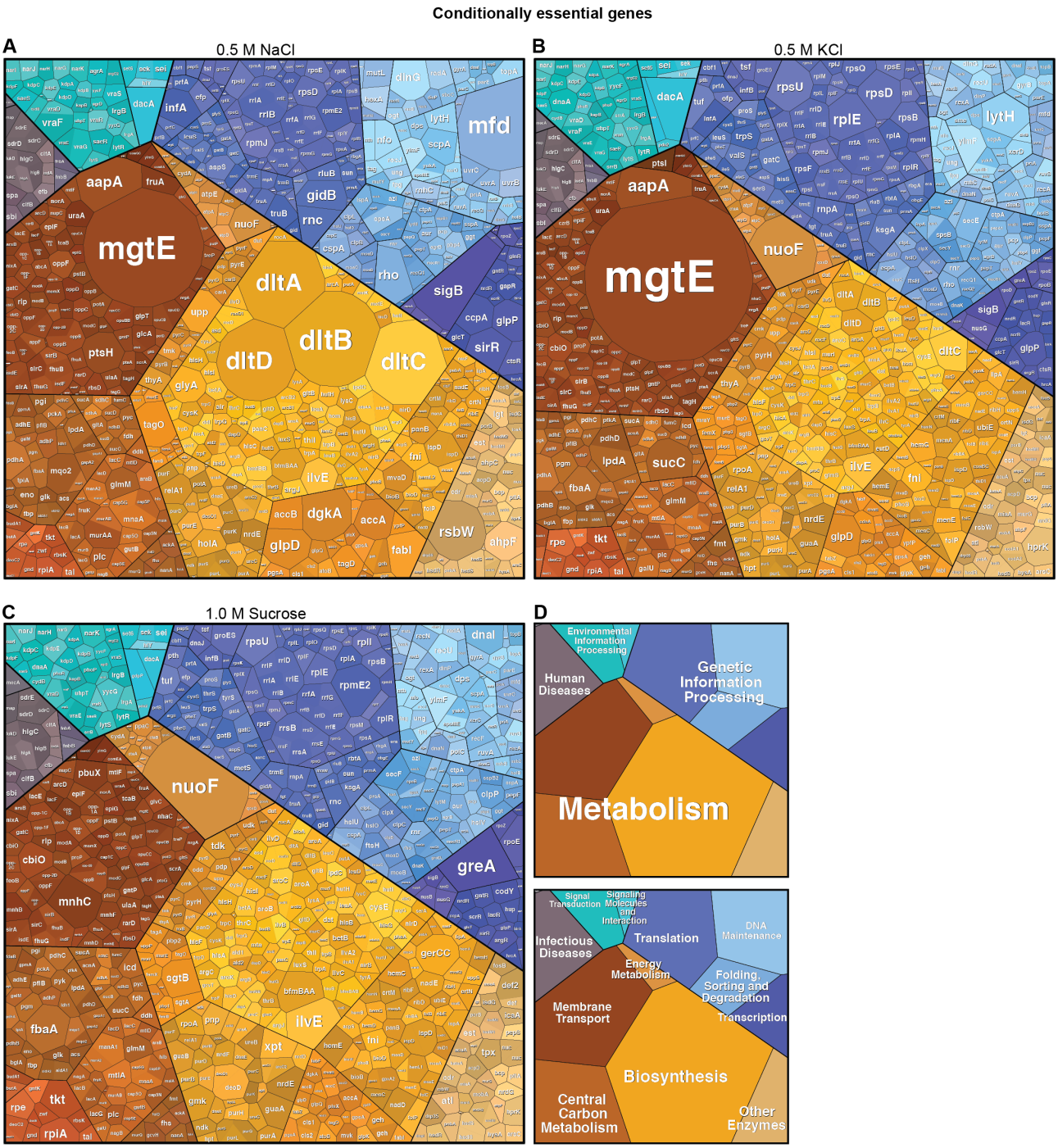

Fig. 8. Voronoi diagram-based visualization of conditionally essential *S. aureus* genes when exposed to different osmotic stressors underlines differences.

Conditionally essential genes of *S. aureus* strains grown either in 0.5 M NaCl (A), 0.5 M KCl (B) or 1.0 M sucrose (C) were mapped to cellular functions. Area sizes were adjusted to their essentiality regardless of p- or q-value to visualize differences on a genome wide level. The larger the area, the

1244 higher the number of transposon insertions in the LBN control condition as compared to the stress

1245 conditions. Colors of polygons indicate cellular functions as detailed in (D).

1246

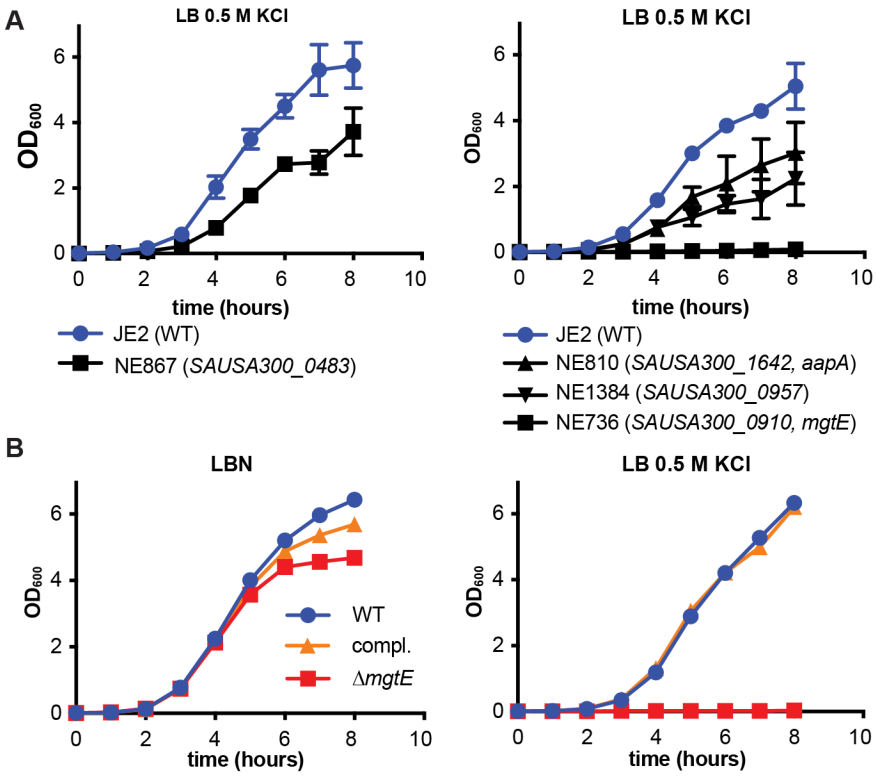

1247

1248 **Fig. 9. Growth curves of putative potassium sensitive mutants in LB containing 0.5 M KCl.**

1249 (A) Growth curves using putative KCl sensitive mutants. *S. aureus* strain JE2 (WT) and strains from
1250 the Nebraska Transposon Mutant Library (NTML) containing transposon insertions in the indicated
1251 and potential KCl essential genes were grown in LB 0.5 M KCl medium and the mean and SDs of the
1252 OD_{600} readings from three biological replicates plotted.

1253 (B) Growth curves using a clean Δ*mgtE* deletion and complementation strain. *S. aureus* strains LAC*
1254 piTET (WT), LAC*Δ*mgtE* piTET (Δ*mgtE*) and the complementation strain LAC*Δ*mgtE* piTET-*mgtE*
1255 (compl.) were grown in LB 0.5 M KCl also containing 100 ng/ml Atet and the mean and SDs of the
1256 OD_{600} readings from three biological replicates were plotted.

1257

1258

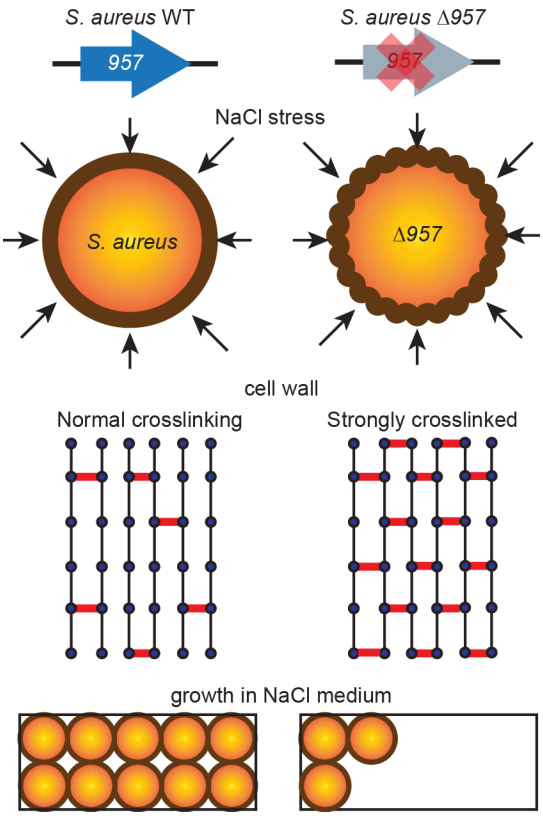

1259 **Fig. 10. Proposed model of 957 activity during NaCl stress.**

1260 *S. aureus* is normally able to grow in medium containing up to 2.5 M NaCl. The deletion of gene *957*
1261 leads to a strong growth defect in high salt conditions and changes in the peptidoglycan structure.
1262 We speculate that the observed increase in peptidoglycan crosslinking will lead to an increased
1263 rigidity of the cell wall and disadvantage and increased cell wall damage when these cells are
1264 exposed to osmotic stress conditions.

1265

1266 **Supplementary Figures**

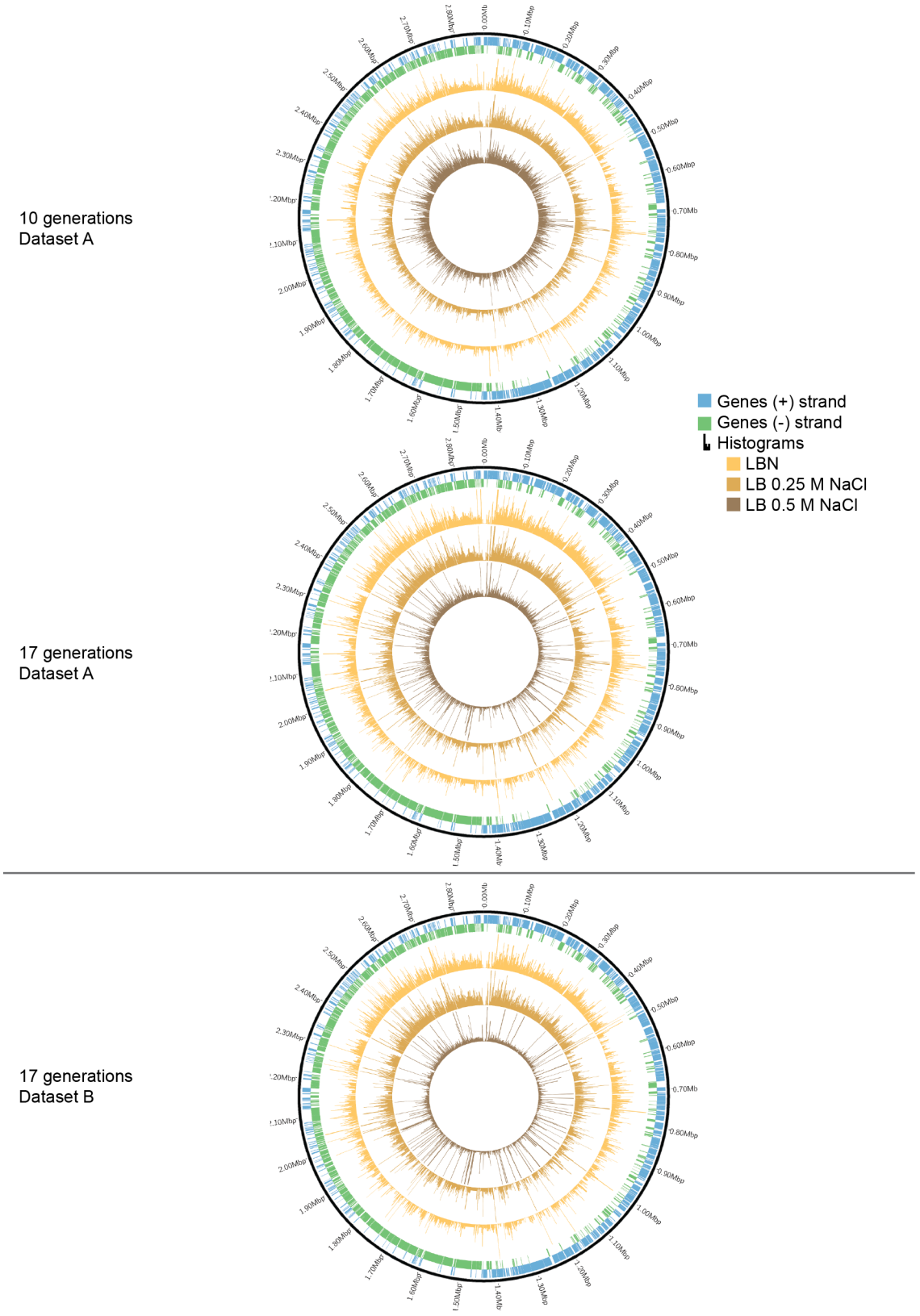

1267

1268 **Supplementary Fig. 1. Circos plots showing transposon insertions in the *S. aureus* genome**
1269 **following growth under different conditions.**

1270 The outer two bands represent genes on the forward (blue) and reverse (green) strand, respectively.
1271 The inner three rings represent transposon insertions per gene following the growth of *S. aureus* in
1272 in either LBN (red), LB 0.25 M NaCl (purple) or LB 0.5 M NaCl (blue). The top two panels are for
1273 dataset A and growth for 10 or 17 generations and the lower panel is for dataset B and growth for
1274 17 generations.
1275

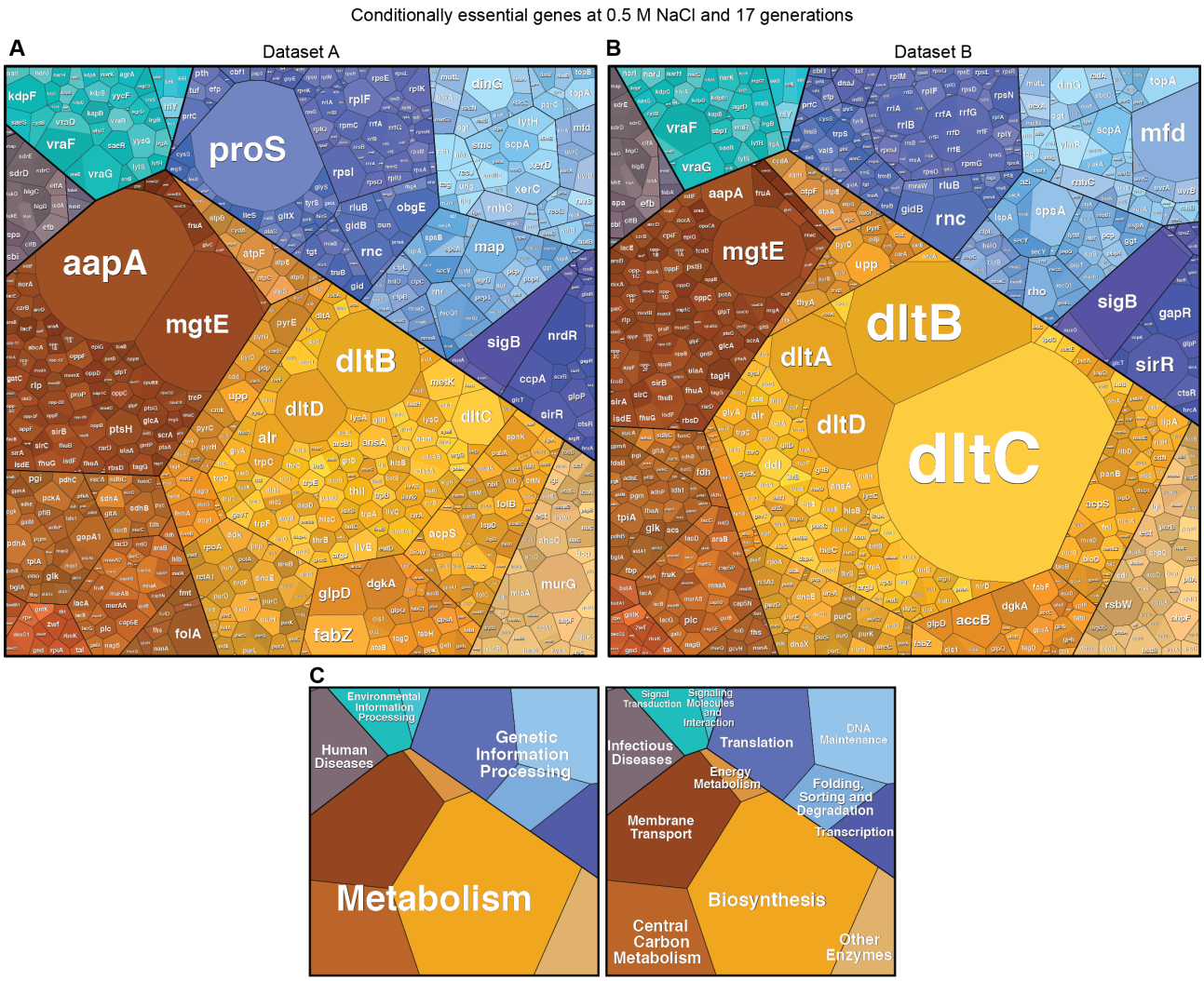

Supplementary Fig. 2. Voronoi diagram-based visualization of *S. aureus* conditionally essential genes when exposed to 0.5 M NaCl.

Conditionally essential *S. aureus* genes from replicate A (A) and replicate B (B) grown in 0.5 M NaCl for 17 generations were mapped to cellular functions with area sizes adjusted to their essentiality regardless of p- or q-value. The larger the area, the lower the number of transposon insertions in stress condition as compared to the LBN control condition. Colors of polygons indicate cellular functions as detailed in (C).

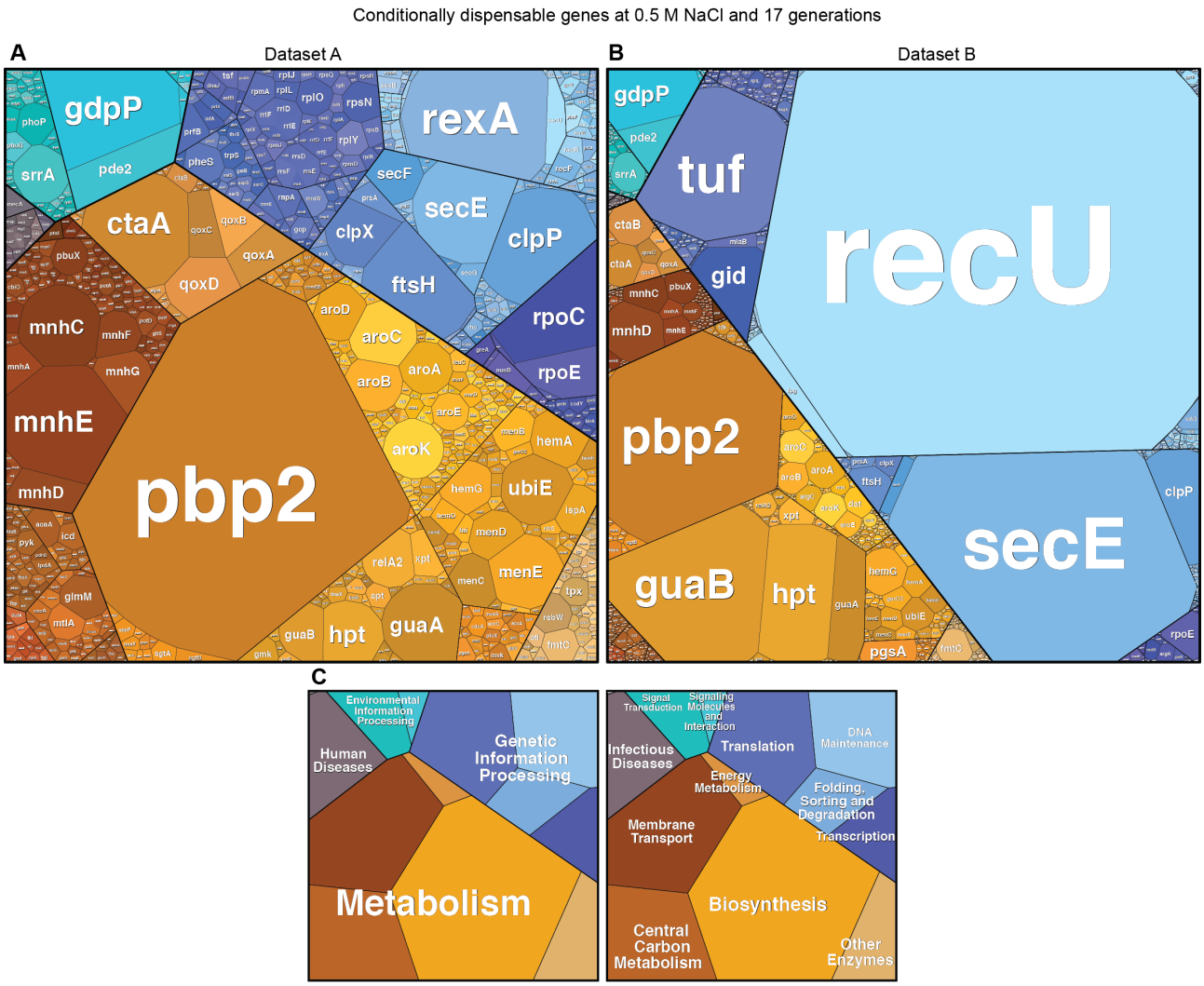

Supplementary Fig. 3. Voronoi diagram-based visualization of *S. aureus* conditionally dispensable genes when exposed to 0.5 M NaCl.

Conditionally dispensable *S. aureus* genes from replicate A (A) and replicate B (B) grown in 0.5 M NaCl for 17 generations were mapped to cellular functions with area sizes adjusted to their dispensability regardless of p- or q-value. The larger the area, the higher the number of transposon insertions in the stress condition as compared to the LBN control. *recU* was scaled to 1/5 of the original ratio to preserve space. Colors of polygons indicate cellular functions as detailed in (C).

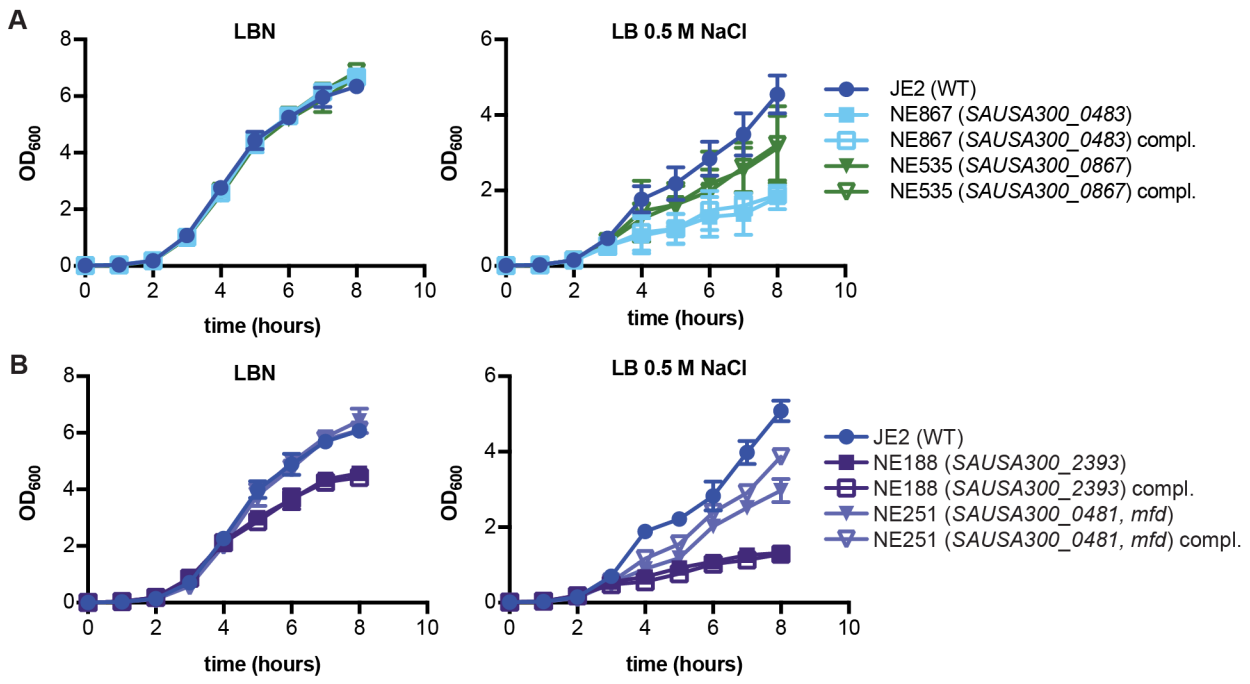

Supplementary Fig. 4. Complementation analysis using *S. aureus* mutants with transposon insertions in putative salt resistance genes.

(A) Growth curves. *S. aureus* strains JE2 (WT), NE867 and NE535 with integrated pCL55 and *S. aureus* strains NE867 and NE535 with respective complementation plasmids were grown in either LBN or LB 0.5 M NaCl and their growth monitored by determining OD_{600} readings.

(B) As in (A) but using strains JE2 piTET (WT) or NE188 and NE251 containing plasmid piTET or the respective complementation plasmid. Strains were grown in LBN or 0.5 M NaCl LB medium supplemented with 100 ng/ml Atet. All experiments were conducted three times and the means and standard deviations were plotted.

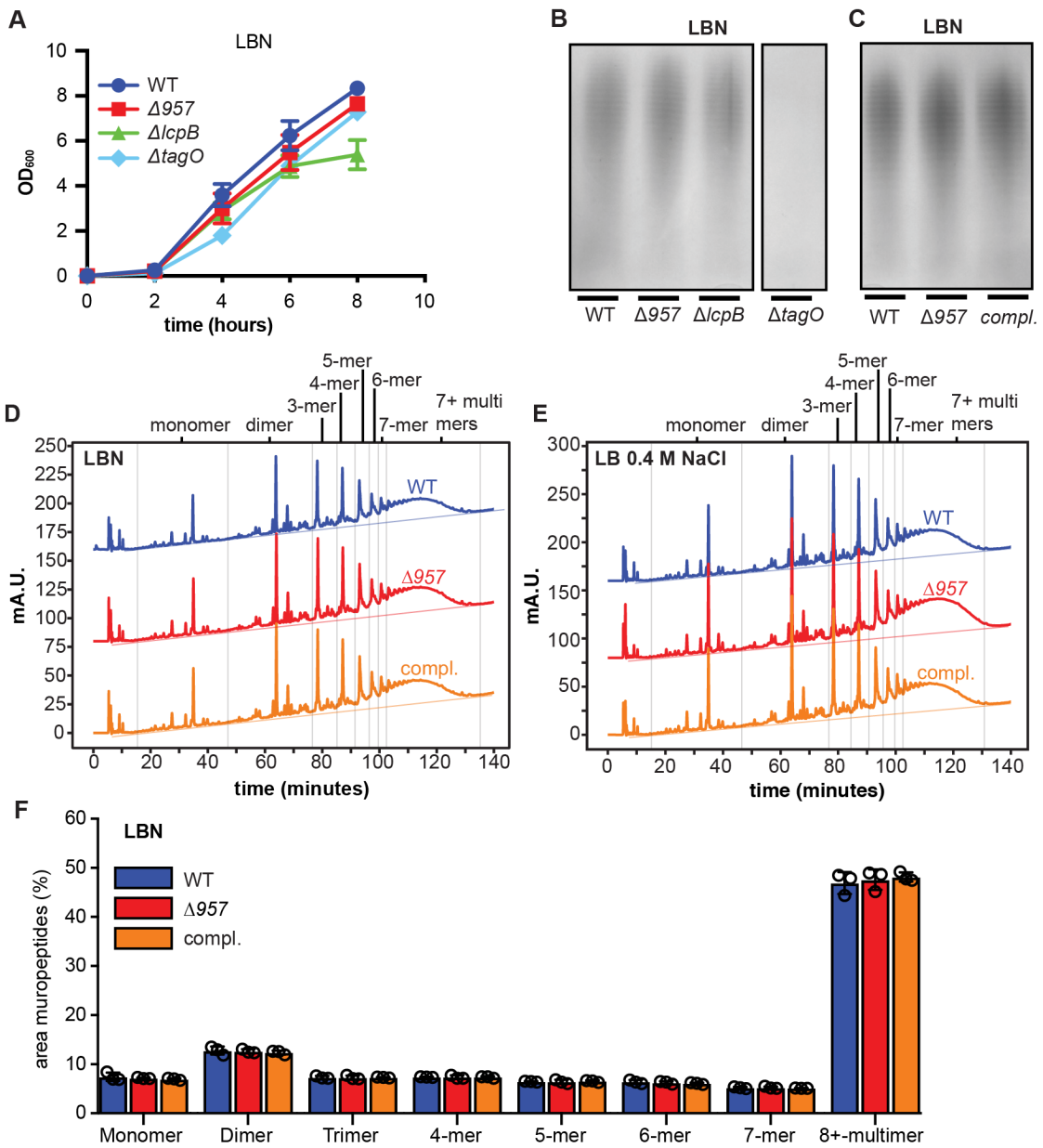

Supplementary Fig. 5. Investigating the involvement of gene *957* in cell wall homeostasis.

(A) Growth curves using strains with mutations in WTA synthesis genes. *S. aureus* strains LAC* (WT), LAC*Δ*957* (Δ*957*), LAC*Δ*lcpB* (Δ*lcpB*) and LAC*Δ*tagO* (Δ*tagO*) were grown in LBN and growth monitored by measuring OD_{600} readings. The experiment was performed three times and means and standard deviations were plotted.

(B) Detection of WTA. WTA was isolated from the strains described in (A) following growth in LBN medium, then subjected to electrophoresis on polyacrylamide gels and visualized by silver staining. One representative result is shown out of three independent experiments.

1313 (C) Detection of WTA. Experimental setup is the same as in (B) but using the strains LAC* piTET (WT),
1314 LAC*Δ*957* piTET (Δ*957*) and LAC* Δ*957* piTET-*957* (compl.).
1315 (D) Muropeptide profile. The same strains as described in panel (C) were grown in LBN medium and
1316 the peptidoglycan isolated, digestion with mutanolysin and the muropeptides subsequently
1317 separated by HPLC. Shown are representative chromatograms from three independent
1318 experiments. Retention time ranges of mono-, di- and higher multi-mers are indicated by vertical
1319 lines.
1320 (E) Muropeptide profiles. As in (D) but bacteria were grown in LB 0.4 M NaCl.
1321 (F) Muropeptide quantification. The areas under the peaks from the chromatograms shown in panel
1322 (D) and two additional replicates were quantified for each mono-, di- or multimer area. Bars
1323 represent mean and error bars standard deviations from three independent experiments. For
1324 statistical analyses, a two-way ANOVA was performed, followed by a Dunnett's post-hoc test but no
1325 significant changes were present between either the wild type and the mutant or the wild type and
1326 the deletion strain. Where induction was necessary, the medium was supplemented with 100 ng/µl
1327 Atet.

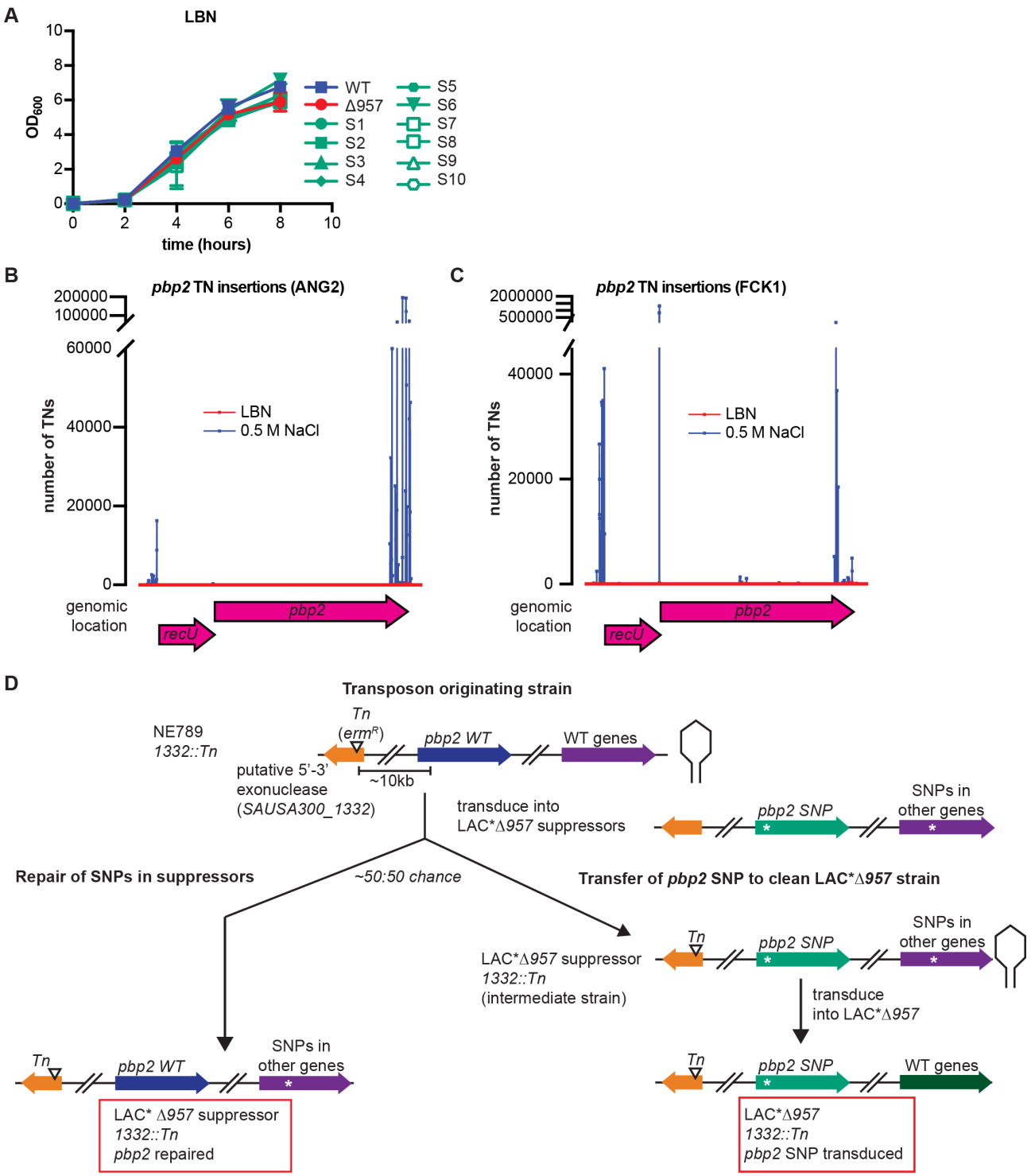

Supplementary Fig. 6. Growth of Δ*957* suppressor strains and schematic of the co-transduction strategy for complementation analysis.

(A) Growth curves of Δ*957* suppressor strains. Strains LAC* (WT), LAC*Δ*957* (Δ*957*) and LAC*Δ*957* suppressors S1 trough S10 (S1-S10) were grown in LBN medium and their growth monitored by

1333 taking OD_{600} readings. The experiment was performed three times and means and standard
1334 deviations were plotted.
1335 (B) TN insertion map. Transposon insertions from replicate A (ANG dataset) were mapped to the
1336 *recU*/*pbp2* operon from a library grown in LBN (red) or LB medium containing 0.5 M NaCl salt (blue).
1337 (C) TN insertion map. As in (B) but using replicate B (FCK dataset).
1338 (D) Schematic of phage co-transduction experiment to either repair the *pbp2* SNP in the suppressor
1339 strains (left branch) or to transduce the *pbp2* suppressor mutations into a clean *957* mutant (right
1340 branch). A phage lysate was prepared using an NTML library strain with a transposon insertion in an
1341 unrelated gene (*SAUSA300_1332*) located approximately 10 kb from the *pbp2* SNPs present in the
1342 suppressor strains. This lysate was used for transductions using different LAC*Δ*957* suppressor
1343 strains as recipient strains. With about 50% frequency, the *pbp2* SNPs were exchanged to the wild
1344 type allele by transducing *SAUSA300_1332*::*Tn* and the WT *pbp2* allele producing strain LAC*Δ*957*
1345 suppressor *1332*::*Tn pbp2* repaired (left branch). In the other cases, the *SAUSA300_1332*::*Tn* region
1346 was transferred to a suppressor strain without replacing the *pbp2* SNP (right branch). A phage lysate
1347 prepared on this intermediate strain (LAC*Δ*957* suppressor *1332*::*Tn*) was then used to transduce
1348 the *pbp2* suppressor SNP into a clean LAC*Δ*957* strain, resulting in the clean suppressor strain
1349 LAC*Δ*957 1332*::Tn *pbp2* SNP transduced.

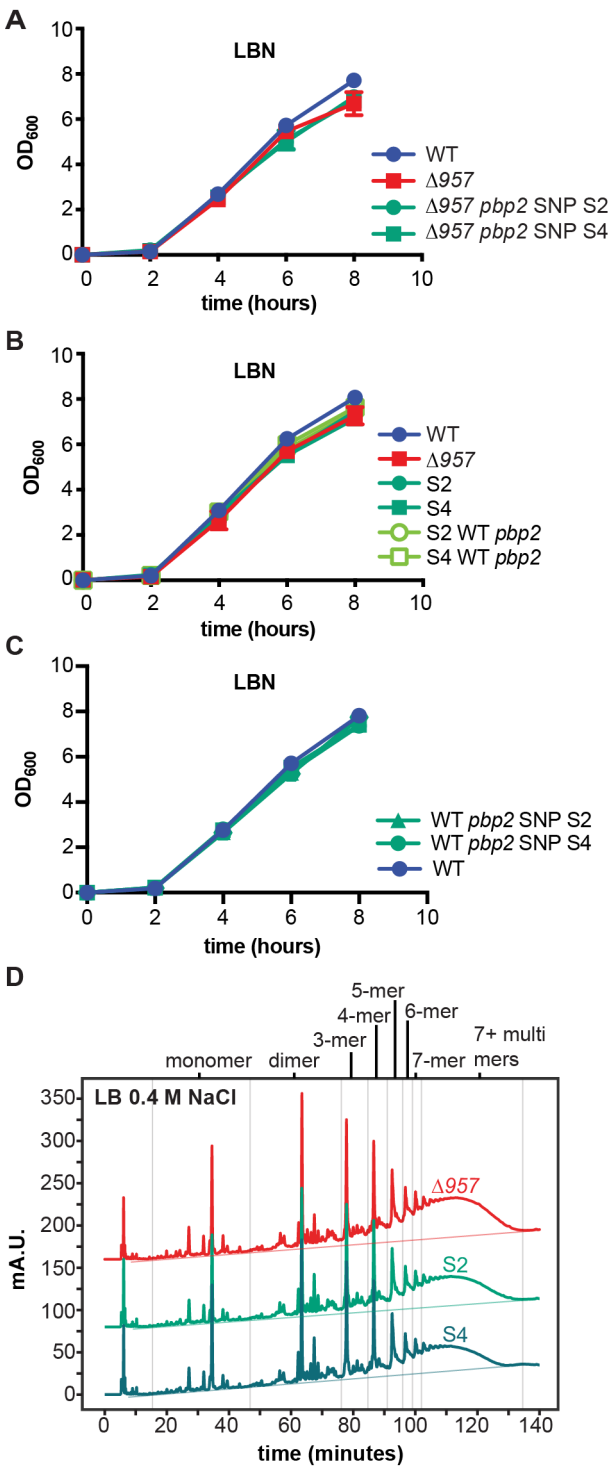

Supplementary Fig. 7. Growth and peptidoglycan analysis of *957* mutant and suppressor strains.

(A) Growth curves using *957* mutants with transduced *pbp2* SNPs. Strains LAC* *1332*::Tn (WT), LAC*Δ*957* *1332*::Tn (Δ*957*), LAC*Δ*957* *1332*::Tn *pbp2* SNP S2 (Δ*957* *pbp2* SNP S2), LAC*Δ*957* suppressor S4 *1332*::Tn (Δ*957* *pbp2* SNP S4) were grown in LBN medium and growth monitored by

1355 determining OD_{600} readings. The means and standard deviations from three independent
1356 experiments were plotted.
1357 (B) Growth curves using *957* suppressor strains carrying a repaired WT *pbp2* gene. Same as in (A)
1358 but using strains LAC* *1332*::Tn (WT), LAC*Δ*957* *1332*::Tn (Δ*957*), LAC*Δ*957* suppressor S2 *1332*::Tn
1359 (S2), LAC*Δ*957* suppressor S4 *1332*::Tn (S4), LAC*Δ*957* suppressor S2 *1332*::Tn repaired WT *pbp2*
1360 (S2 WT *pbp2*), and LAC*Δ*957* suppressor S4 *1332*::Tn repaired WT *pbp2* (S4 WT *pbp2*).
1361 (C) Growth curves using WT strains carrying *pbp2* SNP mutations. Same as in (A) but using strains
1362 LAC* *1332*::Tn (WT), LAC* *1332*::Tn *pbp2* SNP S2 (WT *pbp2* SNP S2) and LAC* *1332*::Tn *pbp2* SNP S4
1363 (WT *pbp2* SNP S4).
1364 (D) Muropeptide profiles. Strains LAC*Δ*957* (Δ*957*), LAC*Δ*957* Suppressor S2 (S2) and S4 LAC*Δ*957*
1365 Suppressor S4 (S4) were grown in LB medium with 0.4 M NaCl, the peptidoglycan was extracted,
1366 digested with mutanolysin, and the muropeptide separated by HPLC. Retention ranges for
1367 monomers, di- and higher oligomers are indicated by vertical lines. The experiment was conducted
1368 with three times and one representative result is shown.

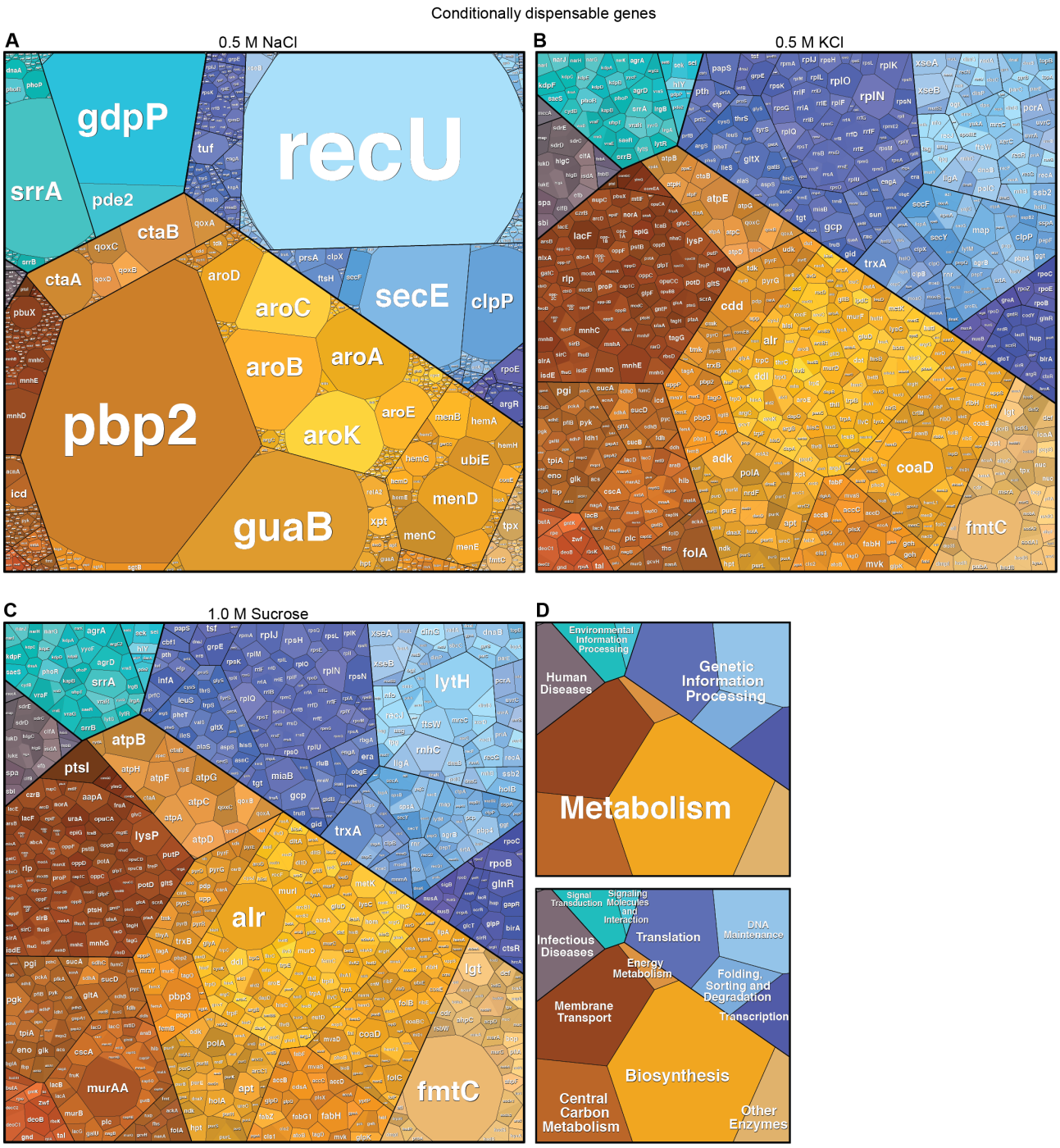

Supplementary Fig. 8. Voronoi diagram-based visualization of conditionally dispensable *S. aureus* genes when exposed to different osmotic stressors.

Conditionally dispensable genes of *S. aureus* strains grown either in 0.5 M NaCl (A), 0.5 M KCl (B) or 1.0 M sucrose (C) were mapped to cellular functions with area sizes adjusted to their essentiality regardless of p- or q-value. The larger the area, the higher the number of transposon insertions in

1375 relation to the LBN control. *recU* was scaled to 1/10 of the original ratio to preserve space. Colors

1376 of polygons indicate cellular functions as detailed in (D).

1377